

Review

Incorporating Hierarchy into Conventional Zeolites for Catalytic Biomass Conversions: A Review

Wasim Khan ¹, Xicheng Jia ¹, Zhijie Wu ² , Jungkyu Choi ³  and Alex C.K. Yip ^{1,*} 

¹ Department of Chemical and Process Engineering, the University of Canterbury, Christchurch 8041, New Zealand; wasim.khan@pg.canterbury.ac.nz (W.K.); xicheng.jia@pg.canterbury.ac.nz (X.J.)

² State Key Laboratory of Heavy Oil Processing and the Key Laboratory of Catalysis of CNPC, China University of Petroleum, Beijing 102249, China; zhijiewu@cup.edu.cn

³ Department of Chemical and Biological Engineering, College of Engineering, Korea University, Seoul 02841, Korea; jungkyu_choi@korea.ac.kr

* Correspondence: alex.yip@canterbury.ac.nz; Tel.: +64-3-3694-086

Received: 14 January 2019; Accepted: 30 January 2019; Published: 31 January 2019



Abstract: Zeolites are promising catalysts that are widely used in petrochemical, oil, and gas industries due to their unique characteristics, such as ordered microporous networks, good hydrothermal stability, large surface area, tunable acidity, and shape-selectivity. Nevertheless, the sole presence of microporous channels in zeolites inevitably restricts the diffusion of bulky reactants and products into and out of the microporous networks, leading to retarded reaction rates or catalyst deactivation. This problem can be overcome by developing hierarchical zeolites which involve mesoporous and macroporous networks. The meso- and macro-porosities can enhance the mass transport of molecules and simultaneously maintain the intrinsic shape selectivity of zeolite microporosity. Hierarchical zeolites are mainly developed through post-synthesis and pre-synthesis or in situ modification of zeolites. In this review, we evaluated both pre-synthesis and post-synthesis modification strategies with more focus on post-synthesis modification strategies. The role of various synthesis strategies on the intrinsic properties of hierarchical zeolites is discussed. The catalytic performance of hierarchical zeolites in important biomass reactions, such as catalytic pyrolysis of biomass feedstock and upgradation of bio-oil, has been summarized. The utilization of hierarchical zeolites tends to give a higher aromatic yield than conventional zeolites with microporosity solely.

Keywords: hierarchical zeolite; synthesis; micropores; mesopores; deactivation; biomass conversion

1. Introduction

Zeolites are hydrated aluminosilicates with an ordered framework, which offers mechanical and thermal stability to zeolites [1]. In addition to mechanical and thermal stability, zeolites possess shape selectivity obtained from their uniform microporous framework (pore size <2 nm) and size exclusion limits imposed on the entry and exit of molecules [2–5]. The unique feature of shape selectivity make zeolites extensively used throughout numerous industries as shape-selective adsorbents and catalysts [6–8]. Moreover, some of the distinct features associated with zeolites include hydrothermal stability, hydrophobicity, high specific surface area, surface acidity or basicity, uniform microporous structure, and coke suppression, i.e., resistant to coke deactivation [9,10]. These features prompt zeolites to be promising candidates for their application in various commercial processes, such as the petrochemical industry, oil refining, pollution abatement, and fine chemistry [11]. Biomass conversion via catalytic pyrolysis and bio-oil upgradation using zeolite catalysts are among the emerging processes that have attracted significant interest in recent years.

Modification of zeolites with mesopores, which enhance accommodation and conversion of bulky molecules, can be achieved via two strategies: (1) pre-synthesis or in situ modification, and (2) post-synthesis modification of conventional zeolites. Each of these strategies have their own advantages and limitations. The most common strategies using post-synthesis modification approach include demetallation, comprising dealumination and desilication. In addition, a recent article reported by Feliczak-Guzik [12] that microwave irradiation and recrystallization are also included in post-synthesis modification strategies. Desilication is also modified by using a surfactant, and thus surfactant-assisted desilication can also be categorized in post-synthesis modification strategy. The pre-synthesis modification or in situ modification strategies include exfoliation, pillaring, templating (using both soft and hard templates), solid zeolitization, and silanization. These strategies are graphically represented in Figure 1.

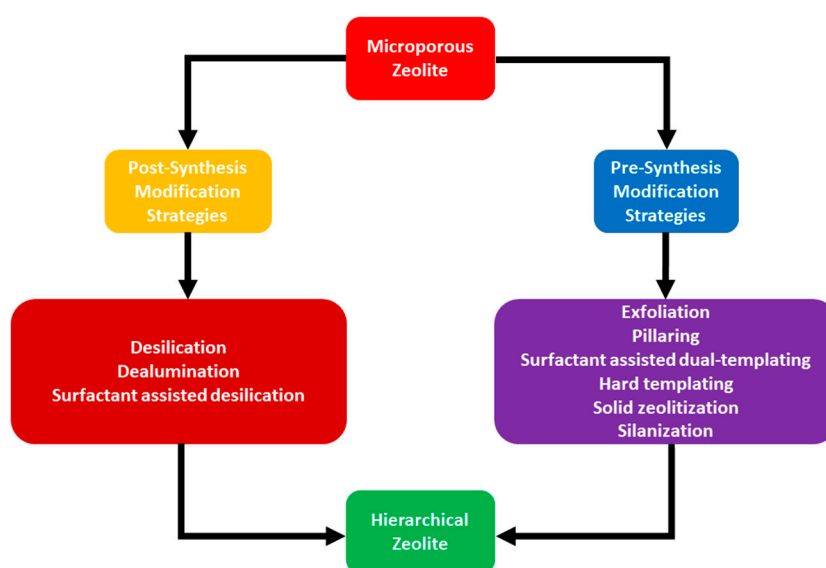


Figure 1. The schematic representation of various hierarchical zeolite formation strategies.

The utilization of conventional fuels and transportation, in particular, has major contribution towards CO₂ emissions, and thus renewable energies have become more important. Biomass is one of the renewable energy sources, which has become popular in recent years and has the potential to produce bio-oil, which can replace fossil fuels [13]. The high production cost and sustainability concerns are among the challenges to deal with when it comes to bio-oil production from biomass [14]. There are various ways to convert the biomass into value-added products, for example, lignocellulosic biomass can be processed through gasification, pyrolysis, hydrolysis, liquefaction, and aqueous phase reforming. The catalytic conversion of biomass involves the cracking of bulky molecules, and therefore conventional zeolites cannot be effective as catalysts. The conventional zeolites comprise micropores, which are not suitable for bulky molecules to diffuse into the inner pores. Moreover, smaller molecules entering the micropores and converting into bulky products are unable to diffuse out of micropores, and thus cause deactivation as active sites are trapped. The modification of zeolite hierarchy offers more pore dimensions for bulky biomass molecules to reach the active sites and come out as products.

The topic of hierarchical zeolites has been discussed and many review articles have also been published in recent years [12,15–20]. The articles reported are focused on either covering the synthesis of hierarchical zeolites as a whole or on specific aspects, such as using hierarchical zeolites as catalysts for certain reactions. Most recently, a review on hierarchical zeolites and its catalytic applications has been published by Feliczak-Guzik [12]. All these articles mainly discuss the significance of hierarchical zeolites from various perspectives. For instance, the recently published article by Feliczak-Guzik [12] reviewed the synthesis strategies and later discussed the application of hierarchical zeolites for two processes, i.e., methanol to hydrocarbon (MTH) conversion and Friedal-Crafts alkylation reactions.

The synthesis of hierarchical zeolites using innovative methods was presented to cover the topic from the view point of how two dimensional zeolite nanosheets contribute in forming hierarchical zeolites [15]. The future of hierarchical zeolites in catalysis was discussed by Yan et al. [16], where the role of shape selectivity and the use of hierarchical zeolites for important gas and liquid phase reactions, such as the Friedal-Crafts reaction, were reviewed. Other review articles discussed the significance of sustainable synthesis and commercial utilization of hierarchical zeolites with both economic and environmental benefits [18,19].

Considering catalytic biomass conversion is an emerging research area and its significance has attracted enormous interest from industry, this review article specifically aims at exploring the methods of preparing hierarchical zeolites and their potential applications in catalytic pyrolysis and bio-oil upgradation.

2. Incorporating Hierarchy to Conventional Zeolites

The incorporation of hierarchical structure into conventional zeolite can be obtained by the generation of either inter- or intra-crystalline mesopores. In addition, hierarchical zeolites may have both micropores and macropores. Hierarchical porosity is mainly influenced by synthesis methods [20]. The secondary porosity introduced in hierarchical zeolites offers improved catalytic performance, which is mainly attributed to diffusion with no impediment, of large compounds into the active sites present inside the channels. It is generally accepted that the rate-controlling step in catalytic reactions using zeolite catalysts is the intra-crystalline transport in the case where bulky molecules are involved. Hierarchical zeolites offer short length of diffusional pathway and thus diffusion limitation can be minimized; this can be elaborated using Knudsen diffusion [21–23]. The hierarchical modification of zeolite is considered to result in less steric hindrance due to the introduction of secondary porosities (mesopores and macropores). Thus, the dimensions of molecules can be increased to a much larger range as needed for a reaction, which extends the application of zeolites to wider areas. Two types of active sites may exist in secondary porosity networks based on their different locations: (i) Active sites accessible from the external surface via secondary channels to the mouth of the microporous network will have almost no steric hindrance; (ii) however, active sites located at the entrance of the microporous network will potentially have a few steric limitations and affect the accessibility of bulky molecules [20]. The shape selectivity of zeolites arising from their ordered microporous network can have a negative impact on product selectivity, e.g., hierarchical zeolites exhibited a decrease in the selectivity of *p*-xylene as compared to conventional zeolites [24,25]. The hierarchical zeolites offer higher resistance to deposition of carbon by either limiting secondary reactions, which mainly contribute to coke formation, or by providing alternative active sites through mesopores. By doing so, deactivation arising from coke deposition is controlled. There are three ways that carbon formation can cause deactivation: (1) coverage of active sites, (2) loss of external surface due to coke deposition, and (3) blockage of micropores [26]. It is generally accepted that micro-sized zeolites are more prone to coke formation than nano-sized zeolites. Hierarchical zeolites are expected to exhibit similar behavior. It is important to note that the secondary porosity in hierarchical zeolites may accommodate more carbon deposits, thus resulting in a higher net coke content compared with the conventional zeolites without mesoporosity [27–30]. Depending on the pore size and diffusional length, bulky molecules can exit the pores readily to prevent coke formation by reducing the diffusional path length or by having appropriate zeolite pore size.

3. Modern Strategies for the Synthesis of Hierarchical Zeolites

Researchers have recently been focusing on developing novel strategies to modify conventional zeolites for synthesizing hierarchical zeolites in order to broaden the scope of their applications. During the last decade, many review articles have been published covering various aspects of the topic i.e., hierarchical zeolite synthesis methods and their applications [17,19,20,31–39]. Moreover, various articles have highlighted the effective approaches for producing secondary mesoporosity without

selective extraction of Al or Si [40–51]. In this section, we aim to evaluate the emerging strategies for the modification of conventional zeolites into hierarchical zeolites and compare the post-synthesis and pre-synthesis or in situ modification strategies. Moreover, the role of these modifications in imparting the unique features that are required of hierarchical zeolites for specific applications is emphasized.

The modification of conventional zeolites to incorporate secondary mesoporosity using pre-synthesis or in situ strategies, or in other words, hydrothermal treatment, can be attained via various methods. The methods involving the use of hard templates require rigid structure-based solid materials, which are introduced into the zeolite mother gel to act as mesoporous or macroporous templates during the zeolite crystallization process. These hard template methods have been an area of extensive research in recent decades. The most commonly studied hard templates are carbonaceous materials due to their structural diversity, readiness to be removed by high temperature treatment, and their chemical inertness. Conversely, the hydrophobicity of carbonaceous materials often narrow the scope of their applications.

On the other hand, soft templates have also been extensively studied for hierarchical zeolite synthesis owing to their flexibility and diversity compared with hard templates. The most frequently used soft template materials include surfactants and polymers. Some of the novel soft templates to incorporate hierarchy or secondary mesoporosity are silanized zeolitic seeds, organosilanes, silylane cationic polymers, and amphiphilic organosilanes. These novel soft templates have been recently developed and recognized as useful and effective methods. For instance, Kresge et al. [52] made the first attempt to use surfactants to produce ordered mesoporous molecular sieves. The idea behind the use of surfactants is associated with the underlying mechanism of micelles formation, which offers a templating effect during crystallization. The surfactant templates are later removed by heat treatment, and thus the space occupied by surfactant molecules converts into mesopores.

The concept of dual templating method is also inspired by the surfactant templates. The use of dual template method to modify the zeolitic materials into hierarchical zeolites by combining the use of structure-directing agents (SDAs) and various surfactants in the zeolite precursor gel has recently been an attraction for researchers. In this method, the surfactants are responsible for templating the mesostructure, while the SDAs build up the whole zeolite along the pore walls of the mesostructure. The synthesis of hierarchical structure using dual templating method was first used soon after [53–55], but problems arose, such as phase-segregation, and the amorphous pore walls of zeolites limited the formation of a successful hierarchical structure. Therefore, numerous modifications, such as the kinetic control of zeolite seeds, usage of cationic polymers, and optimization of reaction conditions, were made to obtain a hierarchical zeolite structure [56–64]. However, these methods offered some disadvantages, including the formation of an insignificant amount of micropores, excessive time consumption, heavily relying on synthesis conditions, and generating a defect-rich structure. Serrano et al. [65] firstly reported the crystallization of silanized zeolite seeds to synthesize hierarchical zeolites. The inspiration of this strategy was taken from previous works [66–69], which were based on the existence of small proto-zeolitic units (approximately 2–5 nm) in the early stages of zeolite crystallization observed in previous studies. Although this method produced hierarchical zeolites with enhanced surface area, porosity, and catalytic activity, the high cost of the SDAs makes this method economically unviable for industrial application.

From the discussion so far, we conclude that the modification of zeolite to introduce secondary porosity using methods or strategies based on pre-synthesis or in situ or hydrothermal treatment offers some advantages and limitations at the same time. The complexity of the process, the economical unviability, and the excessive time consumption are the main hurdles limiting these strategies to be applied on commercial or industrial scale, while better control of structure is one of the main benefits associated with these strategies.

Considering the restrictions associated with pre-synthesis modification strategies, the concept of post-synthesis modification of zeolites in order to incorporate secondary mesoporosity can be considered an alternative approach, which offers advantages over pre-synthesis modification strategies, including simplicity of the process, less time consumption, efficiency, scalability, versatility,

and economic feasibility. These strategies also show disadvantages, such as structural damage and lack of control over mesoporosity generation. The commercial application of post-synthesis modification strategies is another attracting factor which allows researchers to focus on this area of research so that the current industrial catalysts can be improved in terms of efficiency and product selectivity.

The post-synthesis strategies mainly include demetallation, which is composed of dealumination and desilication. As the name indicates, demetallation involves removal of Al or Si atoms from the zeolite framework, which incorporates mesoporosity [70]. The main drawback of demetallation is the structural damage it causes to zeolite. Hydrolysis reactions mainly involved in demetallation are shown in Figure 2. The removal of aluminum from zeolite framework, commonly known as dealumination, is considered to be one of the most useful methods for demetallation. Zeolites with enhanced mesoporosity, high Si/Al ratio, and good stability are extensively reported to be obtained using the dealumination [71–73]. The original purpose for dealumination was to attain stable-structure zeolites with enhanced Si/Al ratio, but unexpected formation of some random mesopores was also reported during dealumination [31].

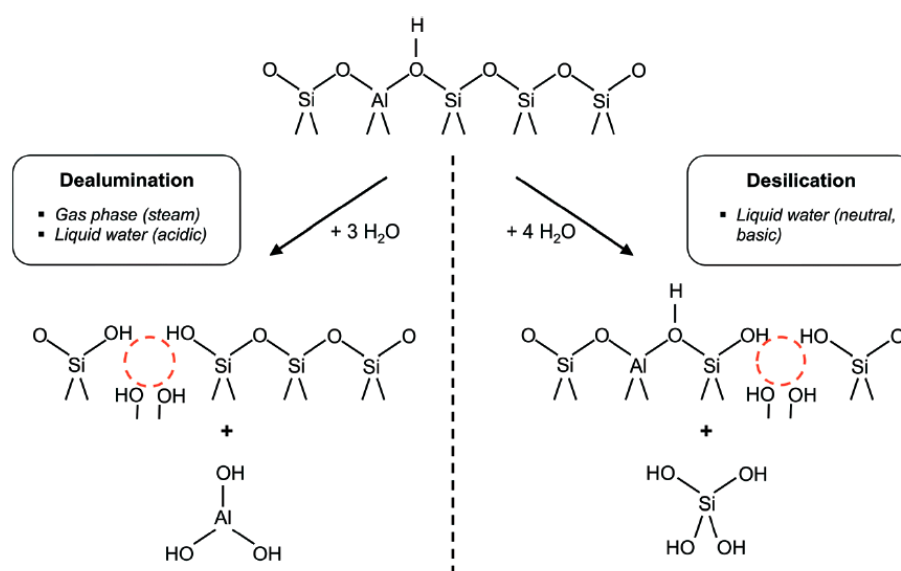


Figure 2. The schematic description of hydrolysis reactions involved in framework demetallation (Adapted from [70]. Copyright 2014 Royal Society of Chemistry).

Dealumination requires hydrolysis of Al-O-Si bonds in the zeolite structure and can be achieved in three ways, including steaming, calcination and acid leaching. The high temperature (>500 °C) steaming process results in the breakdown of Al-O-Si bonds and thus aluminum loss and defects generation takes place simultaneously in the zeolite structure. The loss of aluminum paves way for the movement of less stable silicon to the lost sites and this movement leads to the formation of silanol-rich domains. During the whole described process, many mesopores are formed and part of the amorphous structure is healed at the same time [74]. The formation of debris during the process can deposit on the zeolite surface or inside pores leading to pore blockage and this problem can be addressed by combining steaming method with acid treatment. Various inorganic and organic acids such as nitric acid, hydrochloric acid, tartaric acid etc. have been reported to remove debris [71].

The removal of aluminum using heat treatment also helps to achieve zeolites with increased Brønsted acid sites and stable crystalline structure at temperatures of up to 1000 °C. The use of mild acid is also common after calcination in the case of debris formation [75–77]. The third way to remove aluminum from zeolite structures is acid leaching. The use of acid to remove debris after steaming and calcination has been mentioned earlier, however, the generation of mesopores through aluminum removal using concentrated acids is also reported, and the dealumination via acid leaching depends

upon the zeolite type, nature of acid being used, and pH [28,76,78–83]. The loss of acidity after aluminum extraction, broad range of pore size distribution, and in some cases formation of inactive mesopores inside the channels are among the limitations of dealumination process.

Desilication is another possible way to tailor zeolites with a hierarchical framework by selectively extracting silicon atoms. Figure 3 illustrates the possible mesoporous formation route from desilication [84]. It can be seen from Figure 3a that one crystallite of the parent sample contains several internal Si–OH defects, and Si–OH groups located at the external surface are represented in Figure 3b. Formation of mesopores and removal of internal defects upon alkaline treatment are depicted in Figure 3c,d. Therefore, it can be inferred that Figure 3 gives a general idea about the incorporation of hierarchy or mesoporosity into the conventional zeolite upon alkaline desilication. The generation of mesoporosity using alkaline treatment of zeolites was first reported by Ogura et al. [85], in which it was inferred that mesopores were formed at the expense of dramatically diminished micropores (~40%). The same group later found out that simultaneous extraction of both silica and alumina showed that an alkaline environment favored the extraction of silica more than aluminum from the zeolite framework [86].

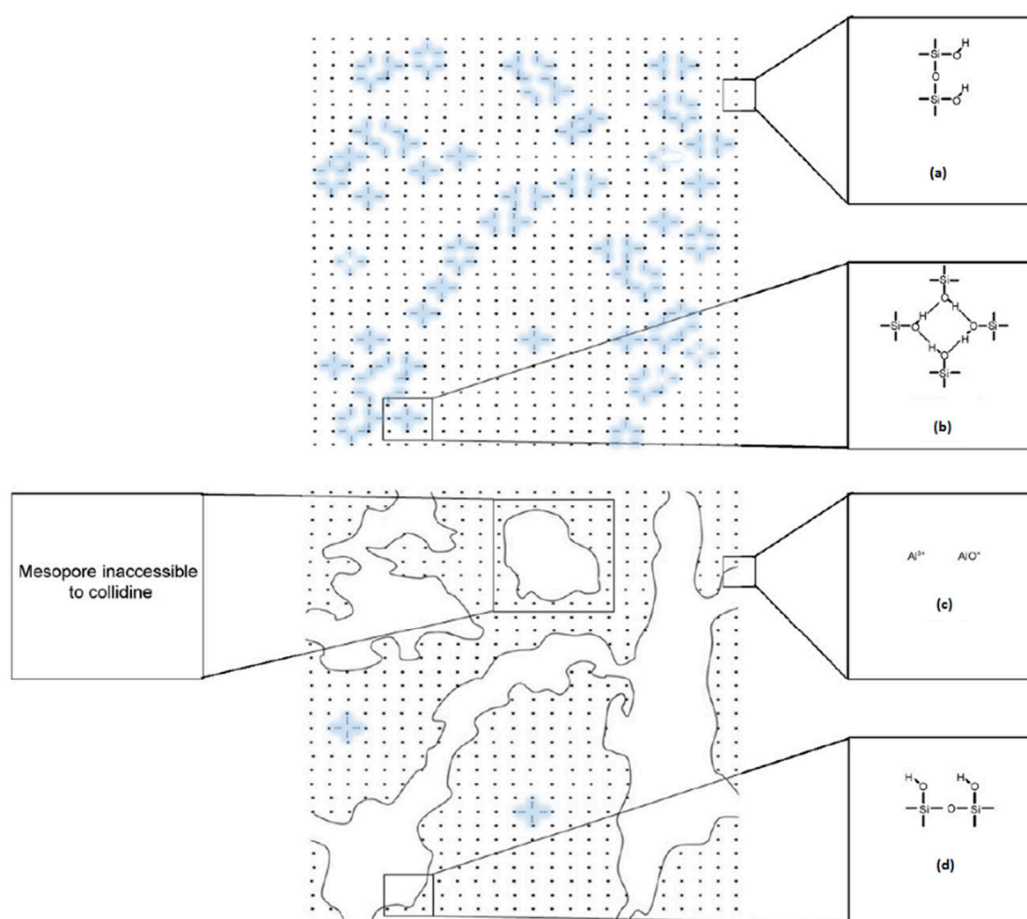


Figure 3. Schematic illustration of the mesopores incorporation to conventional zeolites upon alkaline desilication (Adapted from [84]. Copyright 2009 Elsevier).

The crystallinity of zeolites was reported to be retained, as most of the silica atoms were found to have dissolved from the external surface. The effect of varying alkaline conditions, such as treatment time and alkaline concentrations, was studied and morphological change in ZSM-5 based on these conditions is shown in Figure 4. It can be seen from Figure 4c that the formation of cracks and defects was obvious on the outer surface of zeolites. It was concluded that original microporosity inside ZSM-5 structure was insignificantly influenced by the generation of mesoporosity. The incorporation of mesopores was found to improve the diffusivity, and thus the catalytic performance for cumene cracking.

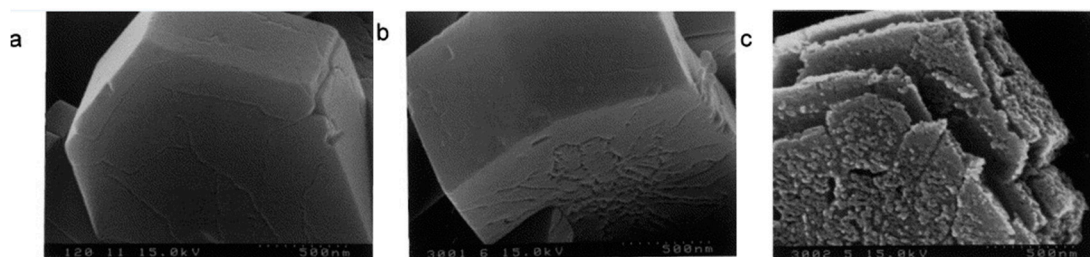


Figure 4. SEM images of alkaline-treated ZSM-5. Treatment was carried out in a 0.1 M NaOH solution at 338 K for (a) 120 min, (b) 300 min, and (c) in a 0.2 M solution at 353 K for 300 min. (Adapted from [86]. Copyright 2001 Elsevier).

The desilication process can be applied to different types of zeolites, e.g., MFI, MTW, MOR, BEA, AST, FER, MWW, IFR, STF, CHA, FAU, TON, and TUN [87–100]. The treatment of zeolites with 0.2 M NaOH solution by keeping the zeolite-to-alkaline solution ratio of ~ 33 g/L for half an hour at 338 K is the most common way to remove silica from the zeolite framework. Desilication from BEA showed that the less stable aluminum in BEA exhibited more silica removal and generated more mesopores than the same method applied to ZSM-5 and mordenite [89]. The comparison between ZSM-22 and MFI when subjected to NaOH treatment showed that ZSM-22 had lower mesopore surface area and desilication efficiency than MFI, due to their morphological differences [99].

Successful desilication using organic hydroxides, such as tetrapropylammonium hydroxide (TPAOH) and tetrabutylammonium hydroxide (TBAOH), has also been documented [101]. The advantage of using an organic base over NaOH is the controllable desilication in the case of organic base as compared to the fast silicon-leaching kinetics in NaOH. Furthermore, the lower selectivity of organic hydroxide for silicon extraction leads to the formation of mesoporous zeolites with higher Si/Al ratios. The synthesis of hierarchical zeolites without severe loss of micropore volume using the modified desilication procedure was also reported [102]. The mass transport and catalytic performance can be improved by using organic cations (TPA^+ or TBA^+) together with NaOH as a pore-growth moderator. It can be concluded that organic hydroxides offer enhanced mesoporosity without severe loss of microporosity, but their high cost as compared to NaOH is one of the limitations in using them at a commercial scale [103].

The formation of hierarchical zeolites via post-synthesis etching and base leaching has recently generated interest. In addition to demetallation, which selectively removes either Al or Si from the zeolite framework, a modern approach that uses bi-fluoride anions to facilitate incorporation of secondary mesoporosity is able to keep most Al and Si in the framework. This approach modifies the conventional zeolite in such a way that the framework composition and the intrinsic acidity of the parent zeolite are mainly retained. Qin et al. [41] published a brief review on this topic and they highlighted the important aspects of the fluoride etching route, which prevents significant changes to the framework composition.

Chen et al. [43] investigated similar post-synthesis fluoride etching for making hierarchical silico-alumino phosphates (SAPO-34). The fluoride etching of SAPO-34 crystals resulted in dissolution of interface between the intergrown crystals and the formation of straight interacting mesopores. The formation of mesopores during fluoride etching did not cause significant change in external surface area. Deposition of extra-framework species was also considered to be negligible. Figure 5 shows the SEM images of the parent and hierarchical SAPO-34, indicating the dissolution of the interface between the crystal domains.

The fluoride treatment significantly influenced the acidity of hierarchical SAPO-34 with a significant loss in Brønsted acid sites. This observation was in contradiction with the work reported by Qin et al. [41], which demonstrated that the intrinsic acidity of the parent zeolite could indeed be retained. On the other hand, a small amount of Lewis acid sites were observed after the fluoride treatment. Despite the significant loss of acidity relative to the parent SAPO-34, hierarchical SAPO-34 gave excellent catalytic activity in the methanol-to-olefin reaction.

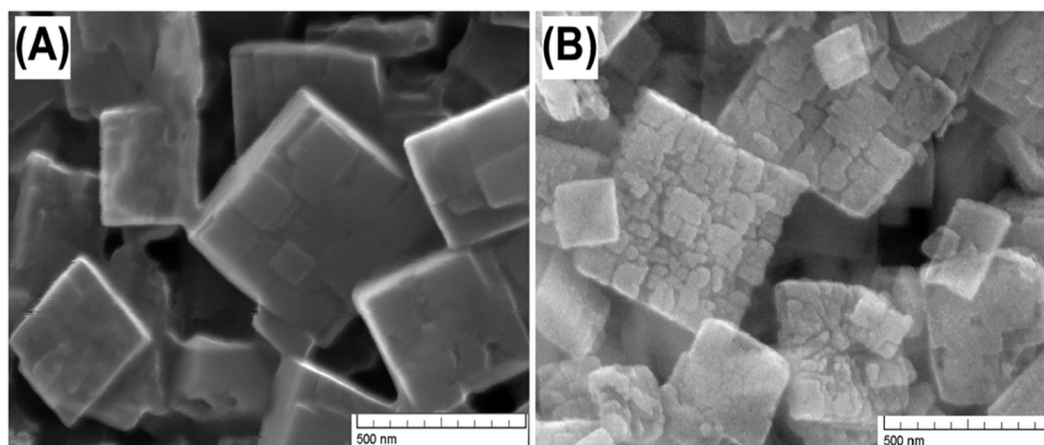


Figure 5. SEM images of (A) parent SAPO-34 and (B) fluoride treated hierarchical SAPO-34. (Adapted from [43]. Copyright 2016 Royal Society of Chemistry).

4. Role of Post-Synthesis Modification Strategies in Biomass Conversion

The conversion of lignocellulosic biomass using fast pyrolysis is an efficient approach that is not only simple but also inexpensive. This approach utilizes renewable feedstock to generate bio-based chemicals and fuels [104–107]. The process thermo-chemically converts solid biomass to solid char, organic vapors, and light gases using high temperatures (500–700 °C). The organic vapors are then condensed to gain the desired bio-based products [108,109]. The use of a zeolite catalyst in the catalytic fast pyrolysis of biomass yields aromatic hydrocarbons, including naphthalene, benzene, toluene, xylene, and naphthalene through various chemical reactions, i.e., oligomerization, cracking, aromatization, and deoxygenation. These aromatic hydrocarbons can be further utilized in the petrochemical or refining industry to generate gasoline-range products [110–114]. The pore size, acid site density, dimensions of the pore network, and presence of large cages are among the main factors that influence the catalytic performance of zeolites in these reactions [115–118].

Various types of zeolites including BEA, FAU, ZSM-5, and mordenite have been employed for fast pyrolysis [35,114,119–122], among which ZSM-5 has been shown to be more efficient than other zeolite types in converting lignocellulosic feedstock such as lignin, cellulose, and woods into higher yields of aromatic products [35,110,119]. Its unique pore structure with moderate pore intersection ($d = 6.36 \text{ \AA}$), pore openings, and steric hindrance makes ZSM-5 suitable for the production of aromatics from biomass and inhibits coking in the pores [35,114,123]. Researchers have also reported that ZSM-5 is not effective in converting some of the bulky oxygenates, such as syringols, which originate from lignocellulose decomposition [35,124]. These oxygenates need to be converted, as they cause corrosion and ageing problems during combustion and storage [105]. The smaller pore size of ZSM-5 compared to the large shape-selective oxygenate impedes the conversion of bulky molecules inside the pores, and thus, limited active sites are available at external surfaces for their conversion. The conversion efficiency could be improved by using large pore size zeolites, such as BEA and FAU zeolites, but pyrolysis in large pores is more favorable for the generation of coke than of aromatics [35,110,114].

The alternative way to improve the conversion efficiency while maintaining a high yield of aromatic is to use hierarchical (or mesoporous) zeolites. ZSM-5 has been reported to contribute effectively when modified to form a hierarchical zeolite catalyst. The mesoporosity of ZSM-5 enhances the conversion of bulky oxygenates, while the capacity to generate aromatics is conserved with its microporosity [35,114]. The details of different strategies to generate hierarchical zeolites are discussed in the previous section. In this section, we address the role of post-synthesis modification strategies to develop hierarchical zeolites, which are utilized in biomass pyrolysis and also in bio-oil upgradation.

Zheng et al. [125] proposed that the main hindrance to the efficient performance of ZSM-5 was slow diffusion of both the reactants and the products in its micropores. To support their hypothesis,

they investigated various sizes of ZSM-5 crystals and correlated size with diffusion path. A comparison between 2 μm , 200 nm, and 50 nm crystals was performed, and the results indicated that the smallest (50 nm) crystals exhibited the highest yield of benzene, toluene, and xylene. Since only three sizes were compared, the data was not enough to make a conclusion, as the results also showed that the 200 nm crystals gave the highest yield of aromatics.

The ZSM-5 catalyst was tailored and a detailed investigation on its crystallinity, porosity, acidity, elemental composition, zeolite structure, and utility for biomass fast pyrolysis was performed [126]. The catalyst was prepared under various hydrothermal conditions (130, 150, 170, and 190 $^{\circ}\text{C}$ for 24 h), and 10 characterization techniques were utilized to study the influence of various parameters, especially crystallinity and extra-framework aluminum, on its catalytic performance. The porosity analysis showed that hydrothermal treatment significantly affected the mesoporosity of the zeolite. The total surface area increased from 372 (for commercial zeolite) to 398–481 m^2/g (for the prepared catalysts). The mesoporosity increased threefold in comparison with that of commercial zeolite. The activity results are shown in Figure 6. It is noteworthy that the catalysts with the highest mesoporosity, i.e., ZSM-5 hydrothermally treated at 130 and 150 $^{\circ}\text{C}$ for 24 h, showed aromatic yields of 15% and 27%, respectively, which are even lower than the aromatics yield of commercial zeolite. This result implies that mesoporosity and smaller size may enhance diffusion but cannot guarantee better yield. Therefore, an optimized catalyst with improved crystallinity and enhanced aluminum insertion in the zeolite framework was prepared and tested. This optimized ZSM-5 catalyst exhibited better performance despite having a lower total surface area, pore volume, and mesoporosity, showing that crystallinity and aluminum insertion played key roles during the pyrolysis reaction.

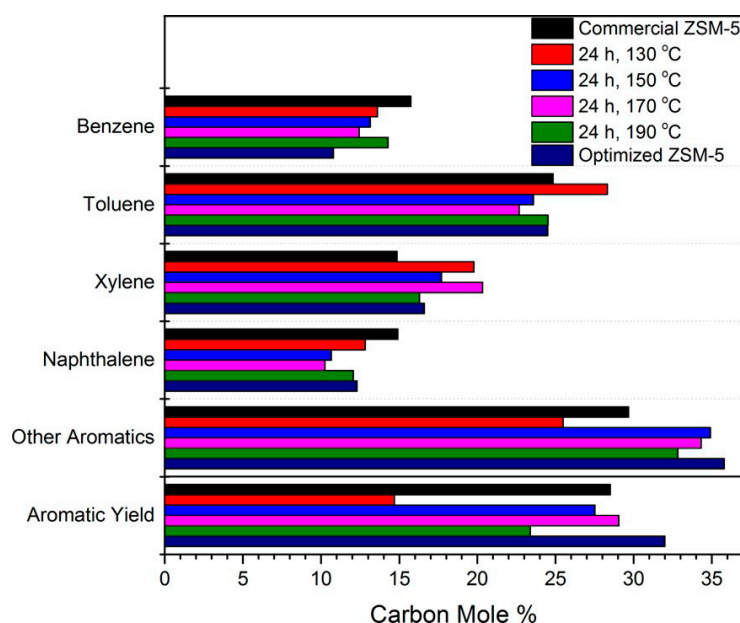


Figure 6. The selectivity and aromatic yield for the catalytic fast pyrolysis of cellulose at 700 $^{\circ}\text{C}$. (Adapted from [126]. Copyright 2016 Wiley-VCH).

The study of the impact of desilication on aluminum-rich ZSM-5 and its consequences on the catalytic pyrolysis of biomass revealed that desilication significantly influenced the acidity, structure, and performance of ZSM-5 [127]. The comprehensive characterization of the resulting zeolites showed that the crystallographic structure, elemental composition, microporosity, and aluminum atom distribution in the framework and extra-framework sites were not greatly influenced by the application of mild desilication conditions to ZSM-5. However, the enhanced mesoporosity increased the Bronsted acid sites by as much as 50%. The SEM images of desilicated ZSM-5 shown in Figure 7 depict the effect of alkali concentration on the surface modification of ZSM-5. A higher alkaline concentration (1 M

NaOH) resulted in visible surface roughness, as well as the formation of larger mesopores. The biomass pyrolysis results revealed that increasing the alkaline concentration from 0.2 M to 1 M resulted in a decrease in activity.

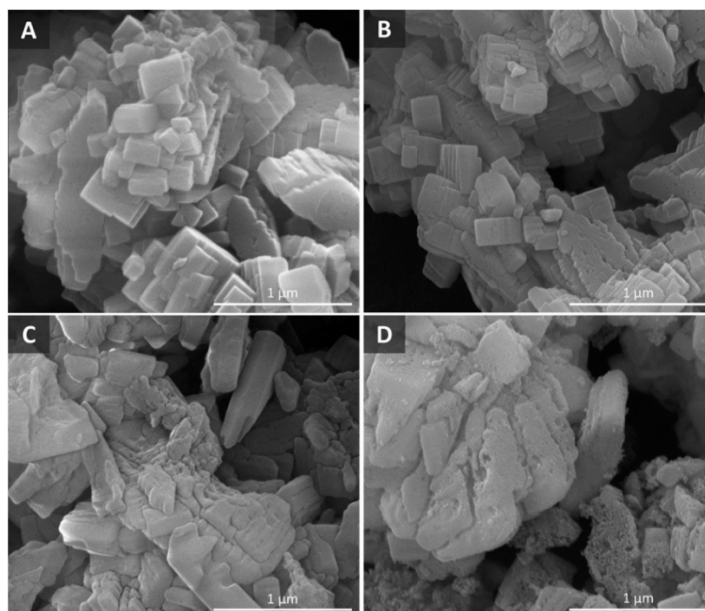


Figure 7. SEM images of (A) untreated ZSM-5, and NaOH-treated ZSM-5 at (B) 0.2 M, (C) 0.5 M, and (D) 1 M. (Adapted from Ref. [127]. Copyright 2017 Elsevier).

The better performance of ZSM-5 treated with a 0.2 M alkaline solution could be attributed to the presence of microporosity in addition to mesoporosity, showing the importance of micropores for the catalytic pyrolysis reaction. Recently, the role of a hierarchical zeolite prepared using a post-synthesis modification strategy, i.e., desilication using NaOH, was elaborated for the catalytic pyrolysis of oak in a microfluidized bed reactor [128]. Furthermore, the coke deposition was extensively investigated to examine the location of coke deposition and its impact on catalytic performance. The activity results indicated that the hierarchical zeolites were more selective towards mono-aromatics, and the selectivity increased twofold after the desilication of the parent zeolite. The better activity results of the hierarchical zeolite could be attributed to the formation of open mesopores during desilication that were large enough for the diffusion of reactants and subsequent products, which could not be achieved in the microporous parent zeolite. Moreover, the larger molecules break down to smaller molecules in the presence of Brønsted acid sites at micropore mouths, and these smaller molecules later produce aromatics, making the hierarchical zeolite shape selective. The energy dispersive x-ray spectroscopy (EDX) study in the TEM revealed the formation of three types of coke in the carbon-deposited zeolites: (A) coke deposition inside the micropores, (B) coke formed on exterior of the crystal surface, and (C) coke precursor trapped in the mesopores. The formation of various coke types versus the biomass-to-catalyst ratio is depicted in Figure 8.

The type of coke formed inside the micropores is more “toxic” than the other two types of coke. The external coke formation mainly relies upon the formation rate of volatiles from wood, their mass transfer to the zeolite surface, their reaction at the external surface, and their internal diffusion into the crystals. This type of coke does not affect the zeolite micropores, which still remain open for reaction. The mesoporosity generated by alkaline treatment paves the way for carbon deposition in the mesopores, thus decreasing the mesopore volume, which in this work occurs at a higher biomass-to-catalyst ratio (0.85). This result depicted greater formation of coke on the outer surface than in the inter-crystal mesopores. Coke generation in the microporous zeolite is the most toxic, as it blocks the micropores. A schematic diagram of the mechanism of coke formation during catalytic pyrolysis is shown in Figure 9.

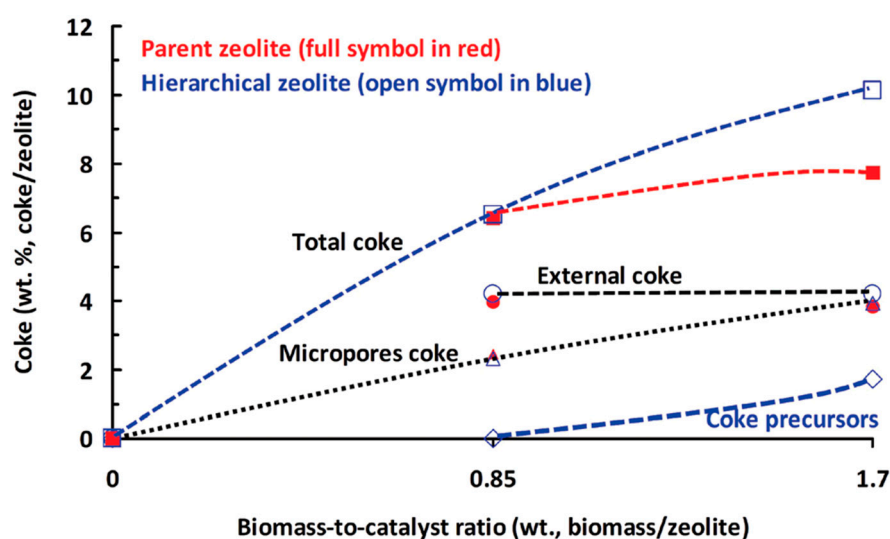


Figure 8. Weight distribution of various coke types as a function of the biomass-to-catalyst ratio. (Adapted from [128]. Copyright 2017 Royal Society of Chemistry).

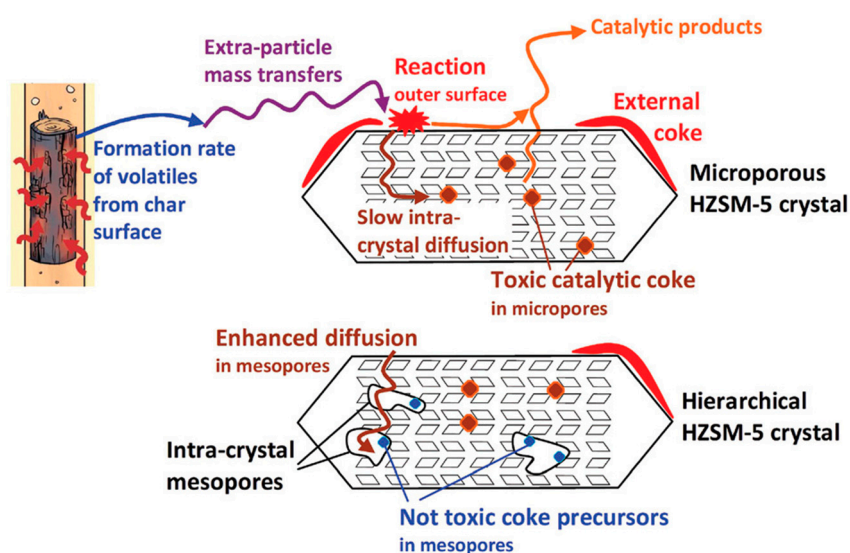


Figure 9. Schematic diagram of the mechanism of coke formation during the catalytic pyrolysis of biomass. (Adapted from [128]. Copyright 2017 Royal Society of Chemistry).

Kabir et al. [129] have recently utilized solid waste (i.e., steel-slag) to prepare mesoporous zeolite using acid and base treatment. The as-synthesized hierarchical zeolite was tested for catalysis of the oil palm mesocarp pyrolysis reaction in a temperature range of 450 to 600 °C. The mesoporous zeolite exhibited a mesopore surface area of 72.9 m²/g, a mesopore volume of 0.45 cm³/g, and an average pore size of 25.51 nm. These textural properties significantly contributed to the conversion of bulky oxygenated compounds obtained from the pyrolysis reaction vapors. The variation in pyrolysis temperature showed a maximum bio-oil yield of 47% at 550 °C, and the products consisted of stable acid-rich carbonyls in higher concentrations than phenolics. The strong acidic surface and higher mesoporosity of the hierarchical zeolite mainly contributed to converting bulky oxygenates to light carbonyls and aromatics.

The role of various alkaline treatments on the catalytic performance of ZSM-5 for cellulose pyrolysis was investigated in a micro-reactor system [130]. ZSM-5 was treated with sodium carbonate (Na₂CO₃), tetrapropylammonium hydroxide (TPAOH), and sodium hydroxide (NaOH). The characterization results showed that the treatment of ZSM-5 with Na₂CO₃ (0.4–0.8 M) presented much more controlled

desilication than the treatment with NaOH. Both the amount and the strength of strong acid sites were enhanced by Na₂CO₃ treatment. The Na₂CO₃ treatment also formed a hierarchical zeolite structure with both micro- and mesoporosity. In contrast, TPAOH affected only the crystallinity of the zeolite, and no change in structure was detected. Higher yields of aromatic hydrocarbons were achieved in Na₂CO₃-treated zeolite than in NaOH-treated zeolite. The aromatics yield increased after Na₂CO₃ treatment and decreased after NaOH treatment, but the opposite trend was observed for the coke yield. The zeolite desilicated with 0.6 M Na₂CO₃ exhibited the maximum yield of aromatics (38.2%) and the minimum coke yield. The strongly acidic nature of Na₂CO₃ treated zeolite shifted the selectivity more towards valuable light aromatics than large aromatics.

Nuttens et al. [122] applied hierarchical zeolites to volarize biomass intermediates (e.g., α -pinene) from turpentine oil. In their study, commercial zeolites, included ultrastable Y (USY), beta, and ZSM-5, were modified using base leaching by NaOH, NH₄OH, diethylamine, and NaOH with tetrapropylammonium bromide. Among the tested commercial zeolites, the introduction of secondary mesoporosity into USY zeolite using diethylamine and NH₄OH was the most successful. The hierarchical USY zeolites exhibited excellent catalytic performance of up to almost 6-fold increase in activity, in the biomass conversion studied due to the significant increase in external surface area.

Ding et al. [131] studied the impact of alkaline concentration during the desilication of HZSM-5 on the catalytic pyrolysis of waste cardboard for aromatics production. The concentration of NaOH used as the alkaline source was varied between 0.1 and 0.7 M. The desilication process at mild alkaline concentrations (≤ 0.3 M) increased the formation of weak acid sites as well as mesopores, while preserving the crystalline structure and micropores of HZSM-5. Higher concentrations of alkaline caused collapse of the crystallinity and micropores of HZSM-5. The combination of retained micropores and mesopores generated during alkaline treatment dramatically enhanced the product yield, and a 44% decrease in coke deposition was observed as well.

The production of aromatics from waste cooking oil over zeolites was studied using catalytic fast pyrolysis [132]. The zeolites were subjected to successive dealumination and desilication and their influence on catalytic activity was investigated. The textural characterization results revealed the formation of mesoporous structure in the modified zeolites. Improvements in both surface area and pore volume was observed after the zeolites were desilicated. The co-existence of micro- and mesoporosity indicated the formation of hierarchical structure during alkaline treatment, but severe alkaline conditions led to micropore loss. The modification time also affected the structure and acidity of the mesoporous zeolites, showing a decreased in the Si/Al ratio as the modification time was increased. Similarly, strong acid sites were replaced with weak acid sites, which were enhanced with increasing modification time. The catalytic performance results showed better aromatics yields over the modified zeolites than over the parent zeolites. Increasing the modification time to 4 h further enhanced the aromatics yield from 42.61 to 58.56%, while further increasing the modification time decreased the yield to 40.96%. This trend could be ascribed to the formation of a suitable synergy between micro- and mesoporosity in the modified zeolite during a moderate modification time of 4 h. Moreover, desilication using NaOH facilitated the formation of mesoporous structure, but the acidity was not improved. The zeolites were further modified by dealumination after desilication, and it was found that the zeolites subjected to desilication followed by dealumination exhibited better performance and product yields.

Bio-oil production from the microwave-assisted catalytic fast pyrolysis of poultry litter using a hierarchical zeolite comprising ZSM-5 and MCM-41 was investigated [133]. The zeolite was subjected to NaOH treatment in which the NaOH concentration varied from 1.5 to 3 mol/L. Hierarchical zeolite were obtained by NaOH leaching, CTAB loading, and finally calcining of the zeolite, thus producing a zeolite composite with MCM-41 as a shell covering ZSM-5 as the core. The results indicated that the shell and core zeolite possessed both microporous and mesoporous structure, and increasing the NaOH concentration increased the surface area as well as the pore volume. The catalytic activity results showed that coke precursors, i.e., large oxygenated molecules, were converted into smaller

compounds in the shell side mesopores induced by increased NaOH concentration. Thus, increasing the NaOH concentration decreased coke formation. The decreased coke formation on the shell side allowed more diffusion of pyrolysis vapor into the internal pores of core ZSM-5, thus enhancing yield of water and gas. The maximum oil fraction was observed when a NaOH concentration of 3 M was used.

The catalytic performance of alkaline-treated zeolite for obtaining biomass-derived furan was investigated, and the impact of the alkaline concentration on the performance and structure of the as-prepared hierarchical zeolite was studied [134]. A moderate alkaline concentration promoted the formation of sheet-like mesopores, which consequently enhanced catalytic activity, but a further increase in the alkaline concentration led to the formation of redundant mesopores. These non-ideal mesopores lowered the access to acid sites, and thus the selectivity; harsh alkaline treatment even collapsed the framework. A concentration of 0.3 M exhibited the best performance among all the tested zeolites prepared at various alkali concentrations. When the hierarchical zeolite with 0.3 M NaOH was subjected to a reaction-regeneration cycle, it exhibited excellent performance even after 20 cycles, showing its long term stability during the reaction.

The catalytic fast pyrolysis of Japanese larch was studied over hierarchical MFI zeolite prepared from amphiphilic organosilane used as the mesopore-directing agent [135]. The performance of the MFI zeolite was compared with that of conventional HZSM-5 and that of mesoporous HZSM-5 derived from HZSM-5. The activity results revealed the excellent performance of hierarchical MFI zeolite for aromatization and deoxygenation. The hierarchical MFI zeolite also exhibited higher selectivity towards valuable aromatics, but the selectivity towards the organic fraction of bio-oil decreased. Moreover, the production of undesired products, i.e., polycyclic aromatic hydrocarbons and a high amount of coke, was observed for the hierarchical MFI zeolite and was attributed to its high mesoporosity.

Stefanidis et al. [136] modified mordenite zeolites using alkaline treatment and studied the role of mesoporous mordenite in biomass pyrolysis. The mesoporosity and crystallinity of mordenite mainly depended upon the strength of the alkaline solution. The Si in mordenite was selectively extracted, and thus, the Si/Al ratio decreased after the alkaline treatment. The catalytic activity results indicated improved performance of mesoporous mordenite in deoxygenation and in the production of better-quality bio-oil. Despite the lower acidity of mesoporous mordenites, synergy among the mesoporosity, high surface area, and high Si/Al ratio contributed to enhancing their catalytic performance.

The product distribution and yield of biomass catalytic pyrolysis were optimized using various types of zeolites [123]. The catalytic performance of mesoporous zeolite was compared with that of other zeolites and found to show a slight improvement in activity. The mesoporous zeolite also promoted the formation of coke, decreased the promotion of monocyclic aromatics, and was found to favor the formation of large aromatics.

The roles of the morphology and mesoporous structure of ZSM-5 were investigated in catalytic fast pyrolysis [29]. ZSM-5 catalysts with various morphologies were tested, and the results indicated positive impacts of mesoporosity and crystallite size on activity. The higher the mesoporosity and the lower the crystallite size, the better were the conversion and the selectivity. A significant reduction in coke formation was also observed after the incorporation of mesoporosity. The micropores were mainly blocked by coke formation, while no coke formation was observed on the exterior or within the mesopores, thus leaving the mesopores available as active sites for reaction.

Lee et al. [137] utilized a combination of both pre-synthesis and post-synthesis strategies to synthesize mesoporous zeolite by modifying commercial zeolites. The resulting aluminosilicates possessed well-developed mesoporosity, controlled aluminum contents, hydrothermal stability, and a suitable distribution of weak and strong acid sites. The mesoporous zeolites were tested for bio-oil upgradation via the catalytic pyrolysis of woody biomass, and their performance was compared with that of other zeolites, such as HZSM-5 and Al-MCM-41. The activity results indicated better performance of the mesoporous

zeolites than the other zeolites. The mesoporous zeolites were lacking in the amount and strength of acid sites due to their disordered framework structure, but their hydrothermal stability significantly contributed to bio-oil upgradation. The mesoporous zeolites retained their performance even after regeneration, showing good reproducibility of their activity results in multiple regeneration cycles.

Table 1 summarizes highlights of hierarchical zeolites studied for catalytic fast pyrolysis of various biomass feedstock. It is noteworthy that some of the conventional zeolites, when transformed into hierarchical zeolites, are found to be less active, and thus the parent zeolites produce more aromatics than modified zeolites.

Table 1. Summary of performance of hierarchical zeolites for catalytic biomass pyrolysis.

Zeolite type	Biomass Feedstock	Aromatics Yield (%)	Coke Yield (%)	Operating Conditions (T (°C), C:F Ratio) ^h	Ref.
Meso ZSM-5	Furan	11.2	3.6	600; -	[29]
ZSM5-optimized	Cellulose	32	-	700; 20:1	[126]
ZSM-5-0.2M ^a	Cellulose	29.4	-	550; 20:1	[127]
ZSM-5-0.2M ^a	Lignin	7.7	-	550; 20:1	[127]
ZSM-5-0.2M ^a	Red oak	27.9	-	550; 20:1	[127]
HZSM-5-0.6M ^b	Cellulose	38.2	27	600; 20:1	[130]
HZSM-5-4h ^c	Waste cooking oil	58.5	-	600; 4:1	[132]
HZSM-5-0.3M ^a	Furan	14.57	7.43	600; -	[134]
ZSM-5-0.3M ^a	Beach wood	30.1	39.9	600; 10:1	[138]
ZSM-5-0.3M ^a	Cellulose	32.1	28.4	600; 10:1	[138]
ZSM-5-0.3M ^a	Lignin	13.2	54.7	600; 10:1	[138]
HZSM-5-0.01MR ^d	Rice straw	26.8	39.2	600; 20:1	[139]
Parent-HZSM-5	Cellulose	34.4	35.1	600; 20:1	[140]
P-HZSM-5-(0.15) ^e	Cellulose	37	28	600; 20:1	[140]
D-HZSM-5-(0.6) ^e	Cellulose	33	38	600; 20:1	[140]
P-ZSM-5(10) ^f	Cellulose	41.8	31	600; 20:1	[141]
HSM-5-0.2M ^a	Rice straw	27.4	35.4	600; 20:1	[142]
ZSM-5-HTS ^g	Cellulose	39.6	27.5	600; 1:20	[143]

Note: ^a xM = Concentration of NaOH for hierarchical zeolite synthesis; ^b xM = Concentration of Na₂CO₃; ^c 4h = Leaching time; ^d 0.01MR = Molar ratio of CTAB/SiO₂; ^e P = pre-crystallized; D = dry gel-based; (0.15) and (0.6) are the sucrose-to-silica ratio; ^f P = 3-(Phenylamino)propyltrimethoxysilane; 10 = amount of organosilane agent; ^g HTS = hexadecyltrimethoxysilane; ^h T = reaction temperature, C:F ratio = catalyst-to-feedstock ratio. Pressure is atmospheric, unless stated otherwise.

The performance assessment for bio-oil upgradation using bottom-up technique based zeolite yielded more mono-aromatics than polycyclic aromatics. This result was mainly attributed to their higher porosity and acidity, which significantly contributed to enhancing the catalytic activity of mesoporous zeolite over that of its parent zeolite [144].

The modification of ZSM-5 by using alkaline desilication to incorporate mesoporosity into the parent zeolite was evaluated for its influence on the composition and yield of bio-oil obtained from the pyrolysis of cellulose and miscanthus [145]. The mesoporous zeolite exhibited better deoxygenation capacity but lower bio-oil yield than the parent zeolite. Moreover, mesoporous zeolite produced small oxygenates from the aldol condensation reaction and higher concentrations of aromatics. The synergistic effect of changes in both the acidity and the porosity of the mesoporous zeolite was the main factor affecting the aromatics yield. The increase in porosity and decrease in acidity both contributed to improving the performance of the mesoporous zeolite in upgrading bio-oil in a bench-scale fixed-bed reactor.

The impact of the interplay between the acidity and porosity of hierarchical zeolites obtained by various techniques on bio-oil upgradation was investigated [146]. Hierarchical zeolites with varying Si/Al ratios were prepared using alkaline desilication and acid washing, and some of the prepared zeolites were subjected to post-synthesis acid treatment. The characterization results indicated that the alkaline and acid treatments significantly influenced the mesoporosity and acidity. A mesopore volume

(V_{meso}) as high as $0.51 \text{ cm}^3/\text{g}$ was obtained for a hierarchical zeolite prepared with successive alkaline treatment and acid washing. The increase in mesoporous surface area also caused an increase in the amount of Brønsted acid sites on the external surface. The catalytic upgradation of bio-oil seemed to be strongly dependent upon the Brønsted acid site density on the mesopore surface, as well as on the extent of mesoporosity incorporated in the hierarchical zeolites. The activity results revealed that the hierarchical zeolites deoxygenated bio-oil via a decarbonylation reaction, while the parent zeolite promoted a dehydration transformation. The presence of a higher amount of Brønsted acid sites at the mesopore surface of hierarchical zeolites greatly promoted the formation of aromatics.

Mohammed et al. probed the performance of microporous and hierarchical mesoporous zeolites for the pyrolytic upgradation of Napier grass [147]. The effects of zeolites on the reaction pathways, product composition, and distribution were also investigated. Two types of hierarchical zeolites were synthesized via desilication using sodium hydroxide concentrations of 0.2 and 0.3 mol/L. The physisorption results indicated the formation of mesopores. The loss of microporous surface area and pore volume also confirmed the formation of mesoporous zeolite. The estimation of the surface acidic sites using temperature-programmed desorption with ammonia as the probe gas showed the existence of strong acid sites in the parent microporous zeolite, while a clear shift from strong acidic sites to weak acidic sites was observed in the modified hierarchical zeolites. The catalytic performance results revealed the positive influence of the hierarchical zeolite on pyrolytic oil upgradation. The hierarchical zeolites enhanced the extent of the deoxygenation reaction, improved the product distribution and contributed to the yield of valuable products from oxygenate transformations. The hierarchical zeolites also produced cycloalkanes and mono-aromatics, in contrast to the parent zeolite, which generated cyclic olefins and polyaromatic hydrocarbons. Moreover, the hierarchical zeolites promoted decarbonylation and decarboxylation, while the parent zeolite mainly favored dehydration. Between the two hierarchical zeolites, the mesoporous zeolite prepared with 0.3 M NaOH exhibited excellent activity and stability, even after four cycles. The product analysis after using the regenerated catalyst revealed a decrease in aromatic hydrocarbon content and an increase in phenol content. The loss in aromatic content was mainly due to the loss of active sites in the regenerated catalyst compared to the fresh catalyst.

The upgradation of bio-oil was studied using an esterification reaction over mesoporous zeolites, which helps to deoxygenate the bio-oil, and thus reduce hydrogen consumption in successive refining steps [148]. The hierarchical zeolites were synthesized using alkaline treatment and acid washing. The physisorption results indicated significant increases in mesopore surface area and pore volume after alkaline treatment. However, interestingly, the micropore volume remained constant, which showed the stability of zeolite framework under the treatment conditions. The esterification reaction over conventional and hierarchical zeolites revealed the significant esterification over zeolites with large pores at lower reaction temperatures (453 K), while medium-pore zeolites exhibited substantial ester formation at slightly higher temperature (473 K). The study of the impact of the Si/Al ratio showed a maximum ester yield over faujasites, while similar yields were obtained over a range of ratios in the case of BEA zeolites. The desilication treatment of the ZSM-5 zeolite resulted in a decrease in acidity and an increase in mesoporosity, which negatively influenced the ester formation in consecutive reaction runs, while the activity remained intact in the case of faujasite zeolites.

Research on the utilization of hierarchical zeolites for biomass conversion is still in progress, seeking to determine a suitable mesoporous structure with appropriate acidity and crystallinity that could pave the way for the effective conversion of biomass into desired products. Further investigation is still required to probe the role of mesoporous structure and crystallinity in the mechanism of biomass conversion to valuable aromatics. The performance of hierarchical zeolites versus conventional zeolites can be graphically represented based on the main products achieved after their use for biomass conversion and pyrolysis (Figure 10).



Figure 10. Comparison of the performances of hierarchical zeolite versus conventional zeolite for biomass conversion and pyrolysis.

5. Summary

The hierarchical zeolites have been an area of interest for researchers in recent years due to their remarkable properties suitable for catalysis, especially for biomass conversion and pyrolysis and bio-oil upgradation. Properties such as their high surface area, uniform microporous structure, significant stability under hydrothermal conditions, tunable acidity, hydrophobic nature, and resistance to coke deactivation make hierarchical zeolites a strong candidate for renewable fuel production, e.g., the production of aromatics from biomass. This review highlighted various ways of introducing mesoporosity into conventional zeolites, and discussed recent articles on biomass pyrolysis and bio-oil upgradation using hierarchical zeolites as catalysts. Mesoporosity allows large biomass molecules to access the active sites within the zeolite structure. Moreover, mesoporosity also helps to promote the formation of valuable products (e.g., monoaromatic hydrocarbons), while large, undesired polyaromatic hydrocarbons are formed over the microporous channels. The mesoporosity is not the only factor contributing to the yield of the desired products, but shape selectivity and the presence of weak acid sites also play vital roles in biomass pyrolysis with valuable outcomes. Various studies have confirmed that hierarchical zeolites with incorporated mesoporosity and elemental composition could not generate the desired product yields, while the product yields were significantly enhanced upon the introduction of weak acidic sites. Both the mesoporosity and acidity contributed prominently to bio-oil upgradation. The prospect of using hierarchical zeolites for biomass pyrolysis and bio-oil upgradation is promising. Detailed studies on the shape selectivity, control of pore size, acidity, and the generation of hierarchical zeolites with multifunctional characteristics should be carried out for biomass conversion and pyrolysis in pilot scale.

Funding: This research received no external funding.

Conflicts of Interest: The authors declare no conflict of interest.

References

1. Flanigen, E.M.; Jansen, J.; van Bekkum, H. *Introduction to Zeolite Science and Practice*; Elsevier: Amsterdam, Netherlands, 1991; Volume 58.
2. Csicsery, S.M. Shape-selective catalysis in zeolites. *Zeolites* **1984**, *4*, 202–213. [[CrossRef](#)]
3. Khouw, C.B.; Davis, M.E. *Shape-Selective Catalysis with Zeolites and Molecular Sieves*; ACS Publications: Washington, DC, USA, 1993.
4. Uguina, M.; Serrano, D.; Van Grieken, R.; Venes, S. Adsorption, acid and catalytic changes induced in ZSM-5 by coking with different hydrocarbons. *Appl. Catal. A Gen.* **1993**, *99*, 97–113. [[CrossRef](#)]
5. Kareem, A.; Chand, S.; Mishra, I. Disproportionation of Toluene to Produce Benzene and p-Xylene—A Review. *J. Sci. Ind. Res.* **2001**, *60*, 319–327.
6. Corma, A. Inorganic solid acids and their use in acid-catalyzed hydrocarbon reactions. *Chem. Rev.* **1995**, *95*, 559–614. [[CrossRef](#)]
7. Marcilly, C.R. Where and how shape selectivity of molecular sieves operates in refining and petrochemistry catalytic processes. *Top. Catal.* **2000**, *13*, 357–366. [[CrossRef](#)]

8. Weitkamp, J. Zeolites and catalysis. *Solid State Ion.* **2000**, *131*, 175–188. [[CrossRef](#)]
9. Rinaldi, R.; Schuth, F. Design of solid catalysts for the conversion of biomass. *Energ. Environ. Sci.* **2009**, *2*, 610–626. [[CrossRef](#)]
10. Serrano-Ruiz, J.C.; Dumesic, J.A. Catalytic routes for the conversion of biomass into liquid hydrocarbon transportation fuels. *Energ. Environ. Sci.* **2011**, *4*, 83–99. [[CrossRef](#)]
11. Perego, C.; Bosetti, A. Biomass to fuels: The role of zeolite and mesoporous materials. *Microporous Mesoporous Mater.* **2011**, *144*, 28–39. [[CrossRef](#)]
12. Feliczak-Guzik, A. Hierarchical zeolites: Synthesis and catalytic properties. *Microporous Mesoporous Mater.* **2018**, *259*, 33–45. [[CrossRef](#)]
13. Swain, P.K.; Das, L.M.; Naik, S.N. Biomass to liquid: A prospective challenge to research and development in 21st century. *Renew. Sustain. Energy Rev.* **2011**, *15*, 4917–4933. [[CrossRef](#)]
14. Fiorese, G.; Catenacci, M.; Verdolini, E.; Bosetti, V. Advanced biofuels: Future perspectives from an expert elicitation survey. *Energy Policy* **2013**, *56*, 293–311. [[CrossRef](#)]
15. Zhang, K.; Ostraat, M.L. Innovations in hierarchical zeolite synthesis. *Catal. Today* **2016**, *264*, 3–15. [[CrossRef](#)]
16. Yan, Y.E.; Guo, X.; Zhang, Y.H.; Tang, Y. Future of nano-/hierarchical zeolites in catalysis: Gaseous phase or liquid phase system. *Catal. Sci. Technol.* **2015**, *5*, 772–785. [[CrossRef](#)]
17. Wei, Y.; Parmentier, T.E.; de Jong, K.P.; Zecevic, J. Tailoring and visualizing the pore architecture of hierarchical zeolites. *Chem. Soc. Rev.* **2015**, *44*, 7234–7261. [[CrossRef](#)] [[PubMed](#)]
18. Verboekend, D.; Perez-Ramirez, J. Towards a Sustainable Manufacture of Hierarchical Zeolites. *ChemSuschem* **2014**, *7*, 753–764. [[CrossRef](#)] [[PubMed](#)]
19. Li, K.; Valla, J.; Garcia-Martinez, J. Realizing the commercial potential of hierarchical zeolites: New opportunities in catalytic cracking. *ChemCatChem* **2014**, *6*, 46–66. [[CrossRef](#)]
20. Serrano, D.P.; Escola, J.M.; Pizarro, P. Synthesis strategies in the search for hierarchical zeolites. *Chem. Soc. Rev.* **2013**, *42*, 4004–4035. [[CrossRef](#)]
21. Christensen, C.H.; Johannsen, K.; Schmidt, I.; Christensen, C.H. Catalytic benzene alkylation over mesoporous zeolite single crystals: Improving activity and selectivity with a new family of porous materials. *J. Am. Chem. Soc.* **2003**, *125*, 13370–13371. [[CrossRef](#)]
22. Christensen, C.H.; Johannsen, K.; Törnqvist, E.; Schmidt, I.; Topsøe, H.; Christensen, C.H. Mesoporous zeolite single crystal catalysts: Diffusion and catalysis in hierarchical zeolites. *Catal. Today* **2007**, *128*, 117–122. [[CrossRef](#)]
23. Jia, X.C.; Jeong, Y.; Baik, H.; Choi, J.; Yip, A.C.K. Increasing resolution of selectivity in alkene hydrogenation via diffusion length in core-shell MFI zeolite. *Catal. Today* **2018**, *314*, 94–100. [[CrossRef](#)]
24. Fernandez, C.; Stan, I.; Gilson, J.P.; Thomas, K.; Vicente, A.; Bonilla, A.; Pérez-Ramírez, J. Hierarchical ZSM-5 Zeolites in Shape-Selective Xylene Isomerization: Role of Mesoporosity and Acid Site Speciation. *Chem.-A Eur. J.* **2010**, *16*, 6224–6233. [[CrossRef](#)] [[PubMed](#)]
25. Musilová, Z.; Žilková, N.; Park, S.-E.; Čejka, J. Aromatic transformations over mesoporous ZSM-5: Advantages and disadvantages. *Top. Catal.* **2010**, *53*, 1457–1469. [[CrossRef](#)]
26. Karge, H. Coke formation on zeolites. *Stud. Surf. Sci. Catal.* **2001**, *137*, 707–746.
27. Srivastava, R.; Choi, M.; Ryoo, R. Mesoporous materials with zeolite framework: Remarkable effect of the hierarchical structure for retardation of catalyst deactivation. *Chem. Commun.* **2006**, 4489–4491. [[CrossRef](#)]
28. Kim, J.; Choi, M.; Ryoo, R. Effect of mesoporosity against the deactivation of MFI zeolite catalyst during the methanol-to-hydrocarbon conversion process. *J. Catal.* **2010**, *269*, 219–228. [[CrossRef](#)]
29. Gou, J.S.; Wang, Z.P.; Li, C.; Qi, X.D.; Vattipalli, V.; Cheng, Y.T.; Huber, G.; Conner, W.C.; Dauenhauer, P.J.; Mountziaris, T.J.; et al. The effects of ZSM-5 mesoporosity and morphology on the catalytic fast pyrolysis of furan. *Green Chem.* **2017**, *19*, 3549–3557. [[CrossRef](#)]
30. Wan, Z.J.; Wu, W.; Chen, W.; Yang, H.; Zhang, D.K. Direct Synthesis of Hierarchical ZSM-5 Zeolite and Its Performance in Catalyzing Methanol to Gasoline Conversion. *Ind. Eng. Chem. Res.* **2014**, *53*, 19471–19478. [[CrossRef](#)]
31. Chal, R.; Gerardin, C.; Bulut, M.; Van Donk, S. Overview and industrial assessment of synthesis strategies towards zeolites with mesopores. *ChemCatChem* **2011**, *3*, 67–81. [[CrossRef](#)]
32. Le Hua, Z.; Zhou, J.; Shi, J.L. Recent advances in hierarchically structured zeolites: Synthesis and material performances. *Chem. Commun.* **2011**, *47*, 10536–10547. [[CrossRef](#)]

33. Lopez-Orozco, S.; Inayat, A.; Schwab, A.; Selvam, T.; Schwieger, W. Zeolitic materials with hierarchical porous structures. *Adv. Mater.* **2011**, *23*, 2602–2615. [[CrossRef](#)] [[PubMed](#)]
34. Verboekend, D.; Pérez-Ramírez, J. Design of hierarchical zeolite catalysts by desilication. *Catal. Sci. Technol.* **2011**, *1*, 879–890. [[CrossRef](#)]
35. Chen, L.-H.; Li, X.-Y.; Rooke, J.C.; Zhang, Y.-H.; Yang, X.-Y.; Tang, Y.; Xiao, F.-S.; Su, B.-L. Hierarchically structured zeolites: Synthesis, mass transport properties and applications. *J. Mater. Chem.* **2012**, *22*, 17381–17403. [[CrossRef](#)]
36. Ivanova, I.I.; Knyazeva, E.E. Micro–mesoporous materials obtained by zeolite recrystallization: Synthesis, characterization and catalytic applications. *Chem. Soc. Rev.* **2013**, *42*, 3671–3688. [[CrossRef](#)] [[PubMed](#)]
37. Möller, K.; Bein, T. Mesoporosity—A new dimension for zeolites. *Chem. Soc. Rev.* **2013**, *42*, 3689–3707. [[CrossRef](#)] [[PubMed](#)]
38. Na, K.; Choi, M.; Ryoo, R. Recent advances in the synthesis of hierarchically nanoporous zeolites. *Microporous Mesoporous Mater.* **2013**, *166*, 3–19. [[CrossRef](#)]
39. Na, K.; Somorjai, G.A. Hierarchically nanoporous zeolites and their heterogeneous catalysis: Current status and future perspectives. *Catal. Lett.* **2015**, *145*, 193–213. [[CrossRef](#)]
40. Catizzzone, E.; Migliori, M.; Aloise, A.; Lamberti, R.; Giordano, G. Hierarchical Low Si/Al Ratio Ferrierite Zeolite by Sequential Postsynthesis Treatment: Catalytic Assessment in Dehydration Reaction of Methanol. *J. Chem.* **2019**, 3084356. [[CrossRef](#)]
41. Qin, Z.X.; Gilson, J.P.; Valtchev, V. Mesoporous zeolites by fluoride etching. *Curr. Opin. Chem. Eng.* **2015**, *8*, 1–6. [[CrossRef](#)]
42. Ivanova, I.I.; Kuznetsov, A.S.; Knyazeva, E.E.; Fajula, F.; Thibault-Starzyk, F.; Fernandez, C.; Gilson, J.P. Design of hierarchically structured catalysts by mordenites recrystallization: Application in naphthalene alkylation. *Catal. Today* **2011**, *168*, 133–139. [[CrossRef](#)]
43. Chen, X.X.; Vicente, A.; Qin, Z.X.; Ruaux, V.; Gilson, J.P.; Valtchev, V. The preparation of hierarchical SAPO-34 crystals via post-synthesis fluoride etching. *Chem. Commun.* **2016**, *52*, 3512–3515. [[CrossRef](#)] [[PubMed](#)]
44. Hu, H.L.; Lyu, J.H.; Rui, J.Y.; Cen, J.; Zhang, Q.F.; Wang, Q.T.; Han, W.W.; Li, X.N. The effect of Si/Al ratio on the catalytic performance of hierarchical porous ZSM-5 for catalyzing benzene alkylation with methanol. *Catal. Sci. Technol.* **2016**, *6*, 2647–2652. [[CrossRef](#)]
45. Lanzafame, P.; Barbera, K.; Papanikolaou, G.; Perathoner, S.; Centi, G.; Migliori, M.; Catizzzone, E.; Giordano, G. Comparison of H⁺ and NH₄⁺ forms of zeolites as acid catalysts for HMF etherification. *Catal. Today* **2018**, *304*, 97–102. [[CrossRef](#)]
46. Martens, J.A.; Verboekend, D.; Thomas, K.; Vanbutsele, G.; Gilson, J.P.; Perez-Ramirez, J. Hydroisomerization of Emerging Renewable Hydrocarbons using Hierarchical Pt/H-ZSM-22 Catalyst. *Chemsuschem* **2013**, *6*, 421–425. [[CrossRef](#)] [[PubMed](#)]
47. Miletto, I.; Paul, G.; Chapman, S.; Gatti, G.; Marchese, L.; Raja, R.; Gianotti, E. Mesoporous Silica Scaffolds as Precursor to Drive the Formation of Hierarchical SAPO-34 with Tunable Acid Properties. *Chem. A Eur. J.* **2017**, *23*, 9952–9961. [[CrossRef](#)] [[PubMed](#)]
48. Van Aelst, J.; Verboekend, D.; Philippaerts, A.; Nuttens, N.; Kurttepel, M.; Gobechiya, E.; Haouas, M.; Sree, S.P.; Denayer, J.F.M.; Martens, J.A.; et al. Catalyst Design by NH₄OH Treatment of USY Zeolite. *Adv. Funct. Mater.* **2015**, *25*, 7130–7144. [[CrossRef](#)]
49. Van Aelst, J.; Haouas, M.; Gobechiya, E.; Houthoofd, K.; Philippaerts, A.; Sree, S.P.; Kirschhock, C.E.A.; Jacobs, P.; Martens, J.A.; Sels, B.F.; et al. Hierarchization of USY Zeolite by NH₄OH. A Postsynthetic Process Investigated by NMR and XRD. *J. Phys. Chem. C* **2014**, *118*, 22573–22582. [[CrossRef](#)]
50. Wang, Z.P.; Dornath, P.; Chang, C.C.; Chen, H.Y.; Fan, W. Confined synthesis of three-dimensionally ordered mesoporous-imprinted zeolites with tunable morphology and Si/Al ratio. *Microporous Mesoporous Mater.* **2013**, *181*, 8–16. [[CrossRef](#)]
51. Catizzzone, E.; Van Daele, S.; Bianco, M.; Di Michele, A.; Aloise, A.; Migliori, M.; Valtchev, V.; Giordano, G. Catalytic application of ferrierite nanocrystals in vapour-phase dehydration of methanol to dimethyl ether. *Appl. Catal. B Environ.* **2019**, *243*, 273–282. [[CrossRef](#)]
52. Kresge, C.; Leonowicz, M.; Roth, W.; Vartuli, J.; Beck, J. Ordered mesoporous molecular sieves synthesized by a liquid-crystal template mechanism. *Nature* **1992**, *359*, 710–712. [[CrossRef](#)]

53. Karlsson, A.; Stöcker, M.; Schmidt, R. Composites of micro- and mesoporous materials: Simultaneous syntheses of MFI/MCM-41 like phases by a mixed template approach. *Microporous Mesoporous Mater.* **1999**, *27*, 181–192. [[CrossRef](#)]
54. Huang, L.; Guo, W.; Deng, P.; Xue, Z.; Li, Q. Investigation of synthesizing MCM-41/ZSM-5 composites. *J. Phys. Chem. B* **2000**, *104*, 2817–2823. [[CrossRef](#)]
55. Petkov, N.; Hözl, M.; Metzger, T.; Mintova, S.; Bein, T. Ordered micro/mesoporous composite prepared as thin films. *J. Phys. Chem. B* **2005**, *109*, 4485–4491. [[CrossRef](#)] [[PubMed](#)]
56. Liu, Y.; Zhang, W.; Pinnavaia, T.J. Steam-stable aluminosilicate mesostructures assembled from zeolite type Y seeds. *J. Am. Chem. Soc.* **2000**, *122*, 8791–8792. [[CrossRef](#)]
57. Liu, Y.; Zhang, W.; Pinnavaia, T.J. Steam-stable MSU-S aluminosilicate mesostructures assembled from zeolite ZSM-5 and zeolite beta seeds. *Angew. Chem. Int. Ed.* **2001**, *40*, 1255–1258. [[CrossRef](#)]
58. Xiao, F.S.; Wang, L.; Yin, C.; Lin, K.; Di, Y.; Li, J.; Xu, R.; Su, D.S.; Schlögl, R.; Yokoi, T. Catalytic properties of hierarchical mesoporous zeolites templated with a mixture of small organic ammonium salts and mesoscale cationic polymers. *Angew. Chem.* **2006**, *118*, 3162–3165. [[CrossRef](#)]
59. Tang, T.; Yin, C.; Wang, L.; Ji, Y.; Xiao, F.-S. Good sulfur tolerance of a mesoporous Beta zeolite-supported palladium catalyst in the deep hydrogenation of aromatics. *J. Catal.* **2008**, *257*, 125–133. [[CrossRef](#)]
60. Song, K.; Guan, J.; Wu, S.; Kan, Q. Synthesis and characterization of strong acidic mesoporous aluminosilicates constructed of zeolite MCM-22 precursors. *Catal. Commun.* **2009**, *10*, 631–634. [[CrossRef](#)]
61. Wang, L.; Zhang, Z.; Yin, C.; Shan, Z.; Xiao, F.-S. Hierarchical mesoporous zeolites with controllable mesoporosity templated from cationic polymers. *Microporous Mesoporous Mater.* **2010**, *131*, 58–67. [[CrossRef](#)]
62. Möller, K.; Yilmaz, B.; Müller, U.; Bein, T. Hierarchical zeolite beta via nanoparticle assembly with a cationic polymer. *Chem. Mater.* **2011**, *23*, 4301–4310. [[CrossRef](#)]
63. Serrano, D.; García, R.; Vicente, G.; Linares, M.; Procházková, D.; Čejka, J. Acidic and catalytic properties of hierarchical zeolites and hybrid ordered mesoporous materials assembled from MFI protozeolitic units. *J. Catal.* **2011**, *279*, 366–380. [[CrossRef](#)]
64. Jin, Y.; Li, Y.; Zhao, S.; Lv, Z.; Wang, Q.; Liu, X.; Wang, L. Synthesis of mesoporous MOR materials by varying temperature crystallizations and combining ternary organic templates. *Microporous Mesoporous Mater.* **2012**, *147*, 259–266. [[CrossRef](#)]
65. Serrano, D.P.; Aguado, J.; Escola, J.M.; Rodríguez, J.M.; Peral, Á. Hierarchical zeolites with enhanced textural and catalytic properties synthesized from organofunctionalized seeds. *Chem. Mater.* **2006**, *18*, 2462–2464. [[CrossRef](#)]
66. Burkett, S.L.; Davis, M.E. Mechanism of structure direction in the synthesis of Si-ZSM-5: An investigation by intermolecular ¹H-²⁹Si CP MAS NMR. *J. Phys. Chem.* **1994**, *98*, 4647–4653. [[CrossRef](#)]
67. Persson, A.; Schoeman, B.; Sterte, J.; Otterstedt, J.-E. The synthesis of discrete colloidal particles of TPA-silicalite-1. *Zeolites* **1994**, *14*, 557–567. [[CrossRef](#)]
68. Schoeman, B.J.; Regev, O. A study of the initial stage in the crystallization of TPA-silicalite-1. *Zeolites* **1996**, *17*, 447–456. [[CrossRef](#)]
69. De Moor, P.-P.E.; Beelen, T.P.; van Santen, R.A. In situ observation of nucleation and crystal growth in zeolite synthesis. A small-angle X-ray scattering investigation on Si-TPA-MFI. *J. Phys. Chem. B* **1999**, *103*, 1639–1650. [[CrossRef](#)]
70. Gounder, R. Hydrophobic microporous and mesoporous oxides as Bronsted and Lewis acid catalysts for biomass conversion in liquid water. *Catal. Sci. Technol.* **2014**, *4*, 2877–2886. [[CrossRef](#)]
71. Zukal, A.; Patzelova, V.; Lohse, U. Secondary porous structure of dealuminated Y zeolites. *Zeolites* **1986**, *6*, 133–136. [[CrossRef](#)]
72. Cooper, D.A.; Hastings, T.W.; Hertzberg, E.P. Process for Preparing Zeolite Y with Increased Mesopore Volume. U.S. Patent US5601798A, 7 September 1997.
73. Sasaki, Y.; Suzuki, T.; Takamura, Y.; Saji, A.; Saka, H. Structure analysis of the mesopore in dealuminated zeolite Y by high resolution TEM observation with slow scan CCD camera. *J. Catal.* **1998**, *178*, 94–100. [[CrossRef](#)]
74. Van Donk, S.; Janssen, A.H.; Bitter, J.H.; de Jong, K.P. Generation, characterization, and impact of mesopores in zeolite catalysts. *Catal. Rev.* **2003**, *45*, 297–319. [[CrossRef](#)]

75. Zhang, C.; Liu, Q.; Xu, Z.; Wan, K. Synthesis and characterization of composite molecular sieves with mesoporous and microporous structure from ZSM-5 zeolites by heat treatment. *Microporous Mesoporous Mater.* **2003**, *62*, 157–163. [[CrossRef](#)]
76. Müller, M.; Harvey, G.; Prins, R. Comparison of the dealumination of zeolites beta, mordenite, ZSM-5 and ferrierite by thermal treatment, leaching with oxalic acid and treatment with SiCl₄ by 1 H, 29 Si and 27 Al MAS NMR. *Microporous Mesoporous Mater.* **2000**, *34*, 135–147. [[CrossRef](#)]
77. Marques, J.P.; Gener, I.; Ayrault, P.; Lopes, J.M.; Ribeiro, F.R.; Guisnet, M. Semi-quantitative estimation by IR of framework, extraframework and defect Al species of HBEA zeolites. *Chem. Commun.* **2004**, *20*, 2290–2291. [[CrossRef](#)] [[PubMed](#)]
78. Barrer, R.; Makki, M. Molecular sieve sorbents from clinoptilolite. *Can. J. Chem.* **1964**, *42*, 1481–1487. [[CrossRef](#)]
79. Meyers, B.; Fleisch, T.; Ray, G.; Miller, J.; Hall, J. A multitechnique characterization of dealuminated mordenites. *J. Catal.* **1988**, *110*, 82–95. [[CrossRef](#)]
80. Lee, G.; Maj, J.; Rocke, S.; Garces, J. Shape selective alkylation of polynuclear aromatics with mordenite-type catalysts: A high yield synthesis of 4,4'-Diisopropylbiphenyl. *Catal. Lett.* **1989**, *2*, 243–247. [[CrossRef](#)]
81. Apelian, M.R.; Fung, A.S.; Kennedy, G.J.; Degnan, T.F. Dealumination of zeolite β via dicarboxylic acid treatment. *J. Phys. Chem.* **1996**, *100*, 16577–16583. [[CrossRef](#)]
82. Lee, E.F.; Rees, L.V. Dealumination of sodium Y zeolite with hydrochloric acid. *J. Chem. Soc. Faraday Trans. 1 Phys. Chem. Condens. Ph.* **1987**, *83*, 1531–1537. [[CrossRef](#)]
83. Giudici, R.; Kouwenhoven, H.; Prins, R. Comparison of nitric and oxalic acid in the dealumination of mordenite. *Appl. Catal. A Gen.* **2000**, *203*, 101–110. [[CrossRef](#)]
84. Holm, M.S.; Svelle, S.; Joensen, F.; Beato, P.; Christensen, C.H.; Bordiga, S.; Bjorgen, M. Assessing the acid properties of desilicated ZSM-5 by FTIR using CO and 2,4,6-trimethylpyridine (collidine) as molecular probes. *Appl. Catal. a-Gen.* **2009**, *356*, 23–30. [[CrossRef](#)]
85. Ogura, M.; Shinomiya, S.-y.; Tateno, J.; Nara, Y.; Kikuchi, E.; Matsukata, M. Formation of uniform mesopores in ZSM-5 zeolite through treatment in alkaline solution. *Chem. Lett.* **2000**, *29*, 882–883. [[CrossRef](#)]
86. Ogura, M.; Shinomiya, S.-y.; Tateno, J.; Nara, Y.; Nomura, M.; Kikuchi, E.; Matsukata, M. Alkali-treatment technique—New method for modification of structural and acid-catalytic properties of ZSM-5 zeolites. *Appl. Catal. A Gen.* **2001**, *219*, 33–43. [[CrossRef](#)]
87. Wei, X.; Smirniotis, P.G. Development and characterization of mesoporosity in ZSM-12 by desilication. *Microporous Mesoporous Mater.* **2006**, *97*, 97–106. [[CrossRef](#)]
88. Groen, J.C.; Sano, T.; Moulijn, J.A.; Pérez-Ramírez, J. Alkaline-mediated mesoporous mordenite zeolites for acid-catalyzed conversions. *J. Catal.* **2007**, *251*, 21–27. [[CrossRef](#)]
89. Groen, J.C.; Abelló, S.; Villaescusa, L.A.; Pérez-Ramírez, J. Mesoporous beta zeolite obtained by desilication. *Microporous Mesoporous Mater.* **2008**, *114*, 93–102. [[CrossRef](#)]
90. Pérez-Ramírez, J.; Abelló, S.; Villaescusa, L.A.; Bonilla, A. Toward Functional Clathrasils: Size-and Composition-Controlled Octadecasil Nanocrystals by Desilication. *Angew. Chem. Int. Ed.* **2008**, *47*, 7913–7917. [[CrossRef](#)]
91. Bonilla, A.; Baudouin, D.; Pérez-Ramírez, J. Desilication of ferrierite zeolite for porosity generation and improved effectiveness in polyethylene pyrolysis. *J. Catal.* **2009**, *265*, 170–180. [[CrossRef](#)]
92. Mokrzycki, Ł.; Sulikowski, B.; Olejniczak, Z. Properties of Desilicated ZSM-5, ZSM-12, MCM-22 and ZSM-12/MCM-41 Derivatives in Isomerization of α -Pinene. *Catal. Lett.* **2009**, *127*, 296. [[CrossRef](#)]
93. de Jong, K.P.; Zečević, J.; Friedrich, H.; de Jongh, P.E.; Bulut, M.; Van Donk, S.; Kenmogne, R.; Finiels, A.; Hulea, V.; Fajula, F. Zeolite Y crystals with trimodal porosity as ideal hydrocracking catalysts. *Angew. Chem.* **2010**, *122*, 10272–10276. [[CrossRef](#)]
94. Musilová-Pavlačková, Z.; Zones, S.I.; Čejka, J. Post-synthesis modification of SSZ-35 zeolite to enhance the selectivity in p-xylene alkylation with isopropyl alcohol. *Top. Catal.* **2010**, *53*, 273–282. [[CrossRef](#)]
95. Sommer, L.; Mores, D.; Svelle, S.; Stöcker, M.; Weckhuysen, B.M.; Olsbye, U. Mesopore formation in zeolite H-SSZ-13 by desilication with NaOH. *Microporous Mesoporous Mater.* **2010**, *132*, 384–394. [[CrossRef](#)]
96. Verboekend, D.; Groen, J.C.; Pérez-Ramírez, J. Interplay of Properties and Functions upon Introduction of Mesoporosity in ITQ-4 Zeolite. *Adv. Funct. Mater.* **2010**, *20*, 1441–1450. [[CrossRef](#)]
97. Kubů, M.; Žilková, N.; Čejka, J. Post-synthesis modification of TUN zeolite: Textural, acidic and catalytic properties. *Catal. Today* **2011**, *168*, 63–70. [[CrossRef](#)]

98. Qin, Z.; Shen, B.; Gao, X.; Lin, F.; Wang, B.; Xu, C. Mesoporous Y zeolite with homogeneous aluminum distribution obtained by sequential desilication–dealumination and its performance in the catalytic cracking of cumene and 1, 3, 5-triisopropylbenzene. *J. Catal.* **2011**, *278*, 266–275. [[CrossRef](#)]
99. Verboekend, D.; Chabaneix, A.M.; Thomas, K.; Gilson, J.-P.; Pérez-Ramírez, J. Mesoporous ZSM-22 zeolite obtained by desilication: Peculiarities associated with crystal morphology and aluminium distribution. *CrystEngComm* **2011**, *13*, 3408–3416. [[CrossRef](#)]
100. Verboekend, D.; Vilé, G.; Pérez-Ramírez, J. Hierarchical Y and USY zeolites designed by post-synthetic strategies. *Adv. Funct. Mater.* **2012**, *22*, 916–928. [[CrossRef](#)]
101. Abello, S.; Bonilla, A.; Perez-Ramirez, J. Mesoporous ZSM-5 zeolite catalysts prepared by desilication with organic hydroxides and comparison with NaOH leaching. *Appl. Catal. A Gen.* **2009**, *364*, 191–198. [[CrossRef](#)]
102. Pérez-Ramírez, J.; Verboekend, D.; Bonilla, A.; Abelló, S. Zeolite Catalysts with Tunable Hierarchy Factor by Pore-Growth Moderators. *Adv. Funct. Mater.* **2009**, *19*, 3972–3979. [[CrossRef](#)]
103. Verboekend, D.; Pérez-Ramírez, J. Desilication Mechanism Revisited: Highly Mesoporous All-Silica Zeolites Enabled Through Pore-Directing Agents. *Chem. -A Eur. J.* **2011**, *17*, 1137–1147. [[CrossRef](#)]
104. Mettler, M.S.; Vlachos, D.G.; Dauenhauer, P.J. Top ten fundamental challenges of biomass pyrolysis for biofuels. *Energ. Environ. Sci.* **2012**, *5*, 7797–7809. [[CrossRef](#)]
105. Huber, G.W.; Iborra, S.; Corma, A. Synthesis of transportation fuels from biomass: Chemistry, catalysts, and engineering. *Chem. Rev.* **2006**, *106*, 4044–4098. [[CrossRef](#)] [[PubMed](#)]
106. Brown, R.C. *Thermochemical Processing of Biomass: Conversion into Fuels, Chemicals and Power*; Wiley: Chichester, UK, 2011.
107. French, R.; Czernik, S. Catalytic pyrolysis of biomass for biofuels production. *Fuel Process. Technol.* **2010**, *91*, 25–32. [[CrossRef](#)]
108. Wang, K.G.; Kim, K.H.; Brown, R.C. Catalytic pyrolysis of individual components of lignocellulosic biomass. *Green Chem.* **2014**, *16*, 727–735. [[CrossRef](#)]
109. Wang, K.G.; Zhang, J.; Shanks, B.H.; Brown, R.C. Catalytic conversion of carbohydrate-derived oxygenates over HZSM-5 in a tandem micro-reactor system. *Green Chem* **2015**, *17*, 557–564. [[CrossRef](#)]
110. Carlson, T.R.; Vispute, T.R.; Huber, G.W. Green gasoline by catalytic fast pyrolysis of solid biomass derived compounds. *Chemsuschem* **2008**, *1*, 397–400. [[CrossRef](#)] [[PubMed](#)]
111. Li, X.Y.; Su, L.; Wang, Y.J.; Yu, Y.Q.; Wang, C.W.; Li, X.L.; Wang, Z.H. Catalytic fast pyrolysis of Kraft lignin with HZSM-5 zeolite for producing aromatic hydrocarbons. *Front. Env. Sci. Eng.* **2012**, *6*, 295–303. [[CrossRef](#)]
112. Kubicka, D.; Kubickova, I.; Cejka, J. Application of Molecular Sieves in Transformations of Biomass and Biomass-Derived Feedstocks. *Catal. Rev.* **2013**, *55*, 1–78. [[CrossRef](#)]
113. Taarning, E.; Osmundsen, C.M.; Yang, X.B.; Voss, B.; Andersen, S.I.; Christensen, C.H. Zeolite-catalyzed biomass conversion to fuels and chemicals. *Energ. Environ. Sci.* **2011**, *4*, 793–804. [[CrossRef](#)]
114. Jae, J.; Tompsett, G.A.; Foster, A.J.; Hammond, K.D.; Auerbach, S.M.; Lobo, R.F.; Huber, G.W. Investigation into the shape selectivity of zeolite catalysts for biomass conversion. *J. Catal.* **2011**, *279*, 257–268. [[CrossRef](#)]
115. Perez-Ramirez, J.; Christensen, C.H.; Egeblad, K.; Christensen, C.H.; Groen, J.C. Hierarchical zeolites: Enhanced utilisation of microporous crystals in catalysis by advances in materials design. *Chem. Soc. Rev.* **2008**, *37*, 2530–2542. [[CrossRef](#)] [[PubMed](#)]
116. Carlson, T.R.; Tompsett, G.A.; Conner, W.C.; Huber, G.W. Aromatic Production from Catalytic Fast Pyrolysis of Biomass-Derived Feedstocks. *Top. Catal.* **2009**, *52*, 241–252. [[CrossRef](#)]
117. He, Y.; Hoff, T.C.; Emdadi, L.; Wu, Y.Q.; Bouraima, J.; Liu, D.X. Catalytic consequences of micropore topology, mesoporosity, and acidity on the hydrolysis of sucrose over zeolite catalysts. *Catal. Sci. Technol.* **2014**, *4*, 3064–3073. [[CrossRef](#)]
118. Emdadi, L.; Wu, Y.Q.; Zhu, G.H.; Chang, C.C.; Fan, W.; Pham, T.; Lobo, R.F.; Liu, D.X. Dual Template Synthesis of Meso- and Microporous MFI Zeolite Nanosheet Assemblies with Tailored Activity in Catalytic Reactions. *Chem. Mater.* **2014**, *26*, 1345–1355. [[CrossRef](#)]
119. Mihalcik, D.J.; Mullen, C.A.; Boateng, A.A. Screening acidic zeolites for catalytic fast pyrolysis of biomass and its components. *J. Anal. Appl. Pyrol.* **2011**, *92*, 224–232. [[CrossRef](#)]
120. Mullen, C.A.; Boateng, A.A. Catalytic pyrolysis-GC/MS of lignin from several sources. *Fuel Process. Technol.* **2010**, *91*, 1446–1458. [[CrossRef](#)]

121. Torri, C.; Reinikainen, M.; Lindfors, C.; Fabbri, D.; Oasmaa, A.; Kuoppala, E. Investigation on catalytic pyrolysis of pine sawdust: Catalyst screening by Py-GC-MIP-AED. *J. Anal. Appl. Pyrol.* **2010**, *88*, 7–13. [[CrossRef](#)]
122. Nuttens, N.; Verboekend, D.; Deneyer, A.; Van Aelst, J.; Sels, B.F. Potential of Sustainable Hierarchical Zeolites in the Valorization of alpha-Pinene. *Chemsuschem* **2015**, *8*, 1197–1205. [[CrossRef](#)] [[PubMed](#)]
123. Foster, A.J.; Jae, J.; Cheng, Y.T.; Huber, G.W.; Lobo, R.F. Optimizing the aromatic yield and distribution from catalytic fast pyrolysis of biomass over ZSM-5. *Appl. Catal. A Gen.* **2012**, *423*, 154–161. [[CrossRef](#)]
124. Fogassy, G.; Thegarid, N.; Schuurman, Y.; Mirodatos, C. From biomass to bio-gasoline by FCC co-processing: Effect of feed composition and catalyst structure on product quality. *Energy Environ. Sci.* **2011**, *4*, 5068–5076. [[CrossRef](#)]
125. Zheng, A.Q.; Zhao, Z.L.; Chang, S.; Huang, Z.; Wu, H.X.; Wang, X.B.; He, F.; Li, H.B. Effect of crystal size of ZSM-5 on the aromatic yield and selectivity from catalytic fast pyrolysis of biomass. *J. Mol. Catal. A Chem.* **2014**, *383*, 23–30. [[CrossRef](#)]
126. Hoff, T.C.; Gardner, D.W.; Thilakaratne, R.; Wang, K.G.; Hansen, T.W.; Brown, R.C.; Tessonnier, J.P. Tailoring ZSM-5 Zeolites for the Fast Pyrolysis of Biomass to Aromatic Hydrocarbons. *Chemsuschem* **2016**, *9*, 1473–1482. [[CrossRef](#)] [[PubMed](#)]
127. Hoff, T.C.; Gardner, D.W.; Thilakaratne, R.; Proano-Aviles, J.; Brown, R.C.; Tessonnier, J.P. Elucidating the effect of desilication on aluminum-rich ZSM-5 zeolite and its consequences on biomass catalytic fast pyrolysis. *Appl. Catal. A Gen.* **2017**, *529*, 68–78. [[CrossRef](#)]
128. Jia, L.Y.; Raad, M.; Hamieh, S.; Toufaily, J.; Hamieh, T.; Bettahar, M.M.; Mauviel, G.; Tarrighi, M.; Pinard, L.; Dufour, A. Catalytic fast pyrolysis of biomass: Superior selectivity of hierarchical zeolites to aromatics. *Green Chem.* **2017**, *19*, 5442–5459. [[CrossRef](#)]
129. Kabir, G.; Mohd Din, A.T.; Hameed, B.H. Pyrolysis of oil palm mesocarp fiber catalyzed with steel slag-derived zeolite for bio-oil production. *Bioresour. Technol.* **2018**, *249*, 42–48. [[CrossRef](#)]
130. Qiao, K.; Shi, X.; Zhou, F.; Chen, H.; Fu, J.; Ma, H.X.; Huang, H. Catalytic fast pyrolysis of cellulose in a microreactor system using hierarchical zsm-5 zeolites treated with various alkalis. *Appl. Catal. A Gen.* **2017**, *547*, 274–282. [[CrossRef](#)]
131. Ding, K.; Zhong, Z.P.; Wang, J.; Zhang, B.; Addy, M.; Ruan, R. Effects of alkali-treated hierarchical HZSM-5 zeolites on the production of aromatic hydrocarbons from catalytic fast pyrolysis of waste cardboard. *J. Anal. Appl. Pyrol.* **2017**, *125*, 153–161. [[CrossRef](#)]
132. Wang, J.; Zhong, Z.P.; Ding, K.; Zhang, B.; Deng, A.D.; Min, M.; Chen, P.; Ruan, R. Successive desilication and dealumination of HZSM-5 in catalytic conversion of waste cooking oil to produce aromatics. *Energy Convers. Manag.* **2017**, *147*, 100–107. [[CrossRef](#)]
133. Zhang, B.; Zhang, J.; Zhong, Z.; Zhang, Y.; Song, M.; Wang, X.; Ding, K.; Ruan, R. Conversion of poultry litter into bio-oil by microwave-assisted catalytic fast pyrolysis using microwave absorbent and hierarchical ZSM-5/MCM-41 catalyst. *J. Anal. Appl. Pyrol.* **2018**. [[CrossRef](#)]
134. Shao, S.S.; Zhang, H.Y.; Shen, D.K.; Xiao, R. Enhancement of hydrocarbon production and catalyst stability during catalytic conversion of biomass pyrolysis-derived compounds over hierarchical HZSM-5. *RSC Adv.* **2016**, *6*, 44313–44320. [[CrossRef](#)]
135. Koo, J.-B.; Jiang, N.; Saravanamurugan, S.; Bejblová, M.; Musilová, Z.; Čejka, J.; Park, S.-E. Direct synthesis of carbon-templating mesoporous ZSM-5 using microwave heating. *J. Catal.* **2010**, *276*, 327–334. [[CrossRef](#)]
136. Stefanidis, S.; Kalogiannis, K.; Iliopoulou, E.F.; Lappas, A.A.; Triguero, J.M.; Navarro, M.T.; Chica, A.; Rey, F. Mesopore-modified mordenites as catalysts for catalytic pyrolysis of biomass and cracking of vacuum gasoil processes. *Green Chem.* **2013**, *15*, 1647–1658. [[CrossRef](#)]
137. Lee, H.I.; Park, H.J.; Park, Y.K.; Hur, J.Y.; Jeon, J.K.; Kim, J.M. Synthesis of highly stable mesoporous aluminosilicates from commercially available zeolites and their application to the pyrolysis of woody biomass. *Catal. Today* **2008**, *132*, 68–74. [[CrossRef](#)]
138. Park, H.J.; Heo, H.S.; Jeon, J.K.; Kim, J.; Ryoo, R.; Jeong, K.E.; Park, Y.K. Highly valuable chemicals production from catalytic upgrading of radiata pine sawdust-derived pyrolytic vapors over mesoporous MFI zeolites. *Appl. Catal. B Environ.* **2010**, *95*, 365–373. [[CrossRef](#)]
139. Asadieraghi, M.; Daud, W.M.A.W. In-situ catalytic upgrading of biomass pyrolysis vapor: Using a cascade system of various catalysts in a multi-zone fixed bed reactor. *Energy Convers. Manag.* **2015**, *101*, 151–163. [[CrossRef](#)]

140. Puertolas, B.; Veses, A.; Callen, M.S.; Mitchell, S.; Garcia, T.; Perez-Ramirez, J. Porosity-Acidity Interplay in Hierarchical ZSM-5 Zeolites for Pyrolysis Oil Valorization to Aromatics. *Chemsuschem* **2015**, *8*, 3283–3293. [[CrossRef](#)] [[PubMed](#)]
141. Li, J.; Li, X.Y.; Zhou, G.Q.; Wang, W.; Wang, C.W.; Komarneni, S.; Wang, Y.J. Catalytic fast pyrolysis of biomass with mesoporous ZSM-5 zeolites prepared by desilication with NaOH solutions. *Appl. Catal. A Gen.* **2014**, *470*, 115–122. [[CrossRef](#)]
142. Zhang, Z.H.; Cheng, H.; Chen, H.; Chen, K.Q.; Lu, X.Y.; Ouyang, P.K.; Fu, J. Enhancement in the aromatic yield from the catalytic fast pyrolysis of rice straw over hexadecyl trimethyl ammonium bromide modified hierarchical HZSM-5. *Bioresour. Technol.* **2018**, *256*, 241–246. [[CrossRef](#)]
143. Chen, H.; Shi, X.; Zhou, F.; Ma, H.X.; Qiao, K.; Lu, X.Y.; Fu, J.; Huang, H. Catalytic fast pyrolysis of cellulose to aromatics over hierarchical nanocrystalline ZSM-5 zeolites prepared using sucrose as a template. *Catal. Commun.* **2018**, *110*, 102–105. [[CrossRef](#)]
144. Qiao, K.; Zhou, F.; Han, Z.; Fu, J.; Ma, H.X.; Wu, G. Synthesis and physicochemical characterization of hierarchical ZSM-5: Effect of organosilanes on the catalyst properties and performance in the catalytic fast pyrolysis of biomass. *Microporous Mesoporous Mater.* **2019**, *274*, 190–197. [[CrossRef](#)]
145. Chen, H.; Cheng, H.; Zhou, F.; Chen, K.Q.; Qiao, K.; Lu, X.Y.; Ouyang, P.K.; Fu, J. Catalytic fast pyrolysis of rice straw to aromatic compounds over hierarchical HZSM-5 produced by alkali treatment and metal-modification. *J. Anal. Appl. Pyrol.* **2018**, *131*, 76–84. [[CrossRef](#)]
146. Chen, H.; Shi, X.; Liu, J.F.; Jie, K.C.; Zhang, Z.H.; Hu, X.B.; Zhu, Y.M.; Lu, X.Y.; Fu, J.; Huang, H.; et al. Controlled synthesis of hierarchical ZSM-5 for catalytic fast pyrolysis of cellulose to aromatics. *J. Mater. Chem. A* **2018**, *6*, 21178–21185. [[CrossRef](#)]
147. Mohammed, I.Y.; Abakr, Y.A.; Yusup, S.; Alaba, P.A.; Morris, K.I.; Sani, Y.M.; Kazi, F.K. Upgrading of Napier grass pyrolytic oil using microporous and hierarchical mesoporous zeolites: Products distribution, composition and reaction pathways. *J. Clean. Prod.* **2017**, *162*, 817–829. [[CrossRef](#)]
148. Milina, M.; Mitchell, S.; Perez-Ramirez, J. Prospectives for bio-oil upgrading via esterification over zeolite catalysts. *Catal. Today* **2014**, *235*, 176–183. [[CrossRef](#)]



© 2019 by the authors. Licensee MDPI, Basel, Switzerland. This article is an open access article distributed under the terms and conditions of the Creative Commons Attribution (CC BY) license (<http://creativecommons.org/licenses/by/4.0/>).